JBC ARTICLE

Truncation of Tau selectively facilitates its pathological activities

Received for publication, January 8, 2020, and in revised form, July 29, 2020 Published, Papers in Press, July 31, 2020, DOI 10.1074/jbc.RA120.012587

Jianlan Gu[1,2,‡], Wen Xu[1,2,‡], Nana Jin[2], Longfei Li[1,2], Yan Zhou[1,2], Dandan Chu[2], Cheng-Xin Gong[1], Khalid Iqbal[1], and Fei Liu[1,*]

From the [1]Department of Neurochemistry, Inge Grundke–Iqbal Research Floor, New York State Institute for Basic Research in Developmental Disabilities, Staten Island, New York, USA, and the [2]Key Laboratory of Neuroregeneration of Jiangsu and Ministry of Education of China, Nantong University, Nantong, Jiangsu, China

Edited by Paul E. Fraser

Neurofibrillary tangles of abnormally hyperphosphorylated Tau are a hallmark of Alzheimer's disease (AD) and related tauopathies. Tau is truncated at multiple sites by various proteases in AD brain. Although many studies have reported the effect of truncation on the aggregation of Tau, these studies mostly employed highly artificial conditions, using heparin sulfate or arachidonic acid to induce aggregation. Here, we report for the first time the pathological activities of various truncations of Tau, including site-specific phosphorylation, self-aggregation, binding to hyperphosphorylated and oligomeric Tau isolated from AD brain tissue (AD O-Tau), and aggregation seeded by AD O-Tau. We found that deletion of the first 150 or 230 amino acids (aa) enhanced Tau's site-specific phosphorylation, self-aggregation, and binding to AD O-Tau and aggregation seeded by AD O-Tau, but deletion of the first 50 aa did not produce a significant effect. Deletion of the last 50 aa was found to modulate Tau's site-specific phosphorylation, promote its self-aggregation, and cause it to be captured by and aggregation seeded by AD O-Tau, whereas deletion of the last 20 aa had no such effects. Among the truncated Taus, $Tau_{151–391}$ showed the highest pathological activities. AD O-Tau induced aggregation of $Tau_{151–391}$ *in vitro* and in cultured cells. These findings suggest that the first 150 aa and the last 50 aa protect Tau from pathological characteristics and that their deletions facilitate pathological activities. Thus, inhibition of Tau truncation may represent a potential therapeutic approach to suppress Tau pathology in AD and related tauopathies.

Tau is a major neuronal microtubule-associated protein. Aggregation of Tau into neurofibrillary tangles (NFTs) is a hallmark brain lesion of Alzheimer's disease (AD) and related tauopathies (1–4). The number of NFTs correlates with the severity of dementia (5–7), and the regional distribution of Tau pathology is apparently associated with the progression of AD (8, 9).

In AD brain, Tau is abnormally hyperphosphorylated at many sites (10–12). Hyperphosphorylation of Tau leads to its loss of normal function, gain of neurotoxicity, and aggregation into NFTs (13–15). Tau pathology can be induced in the mouse brain by injection of Tau aggregates isolated from AD or Tau transgenic mouse brains or produced *in vitro* (16–20). Abnormally hyperphosphorylated and cytosolic Tau isolated from AD brain (AD P-Tau) by sedimentation and ion-exchange chromatography (10) can sequester/capture normal Tau and template it into filaments *in vitro* (13). We recently found that like AD P-Tau, oligomeric Tau isolated from AD brain (AD O-Tau) by sedimentation also effectively induces Tau aggregation in cultured cells (21) and templates Tau pathology *in vivo* (22–24) in a prion-like fashion, which may underlie the amplification and propagation of Tau pathology throughout AD brain.

In addition to hyperphosphorylation, Tau is abnormally truncated at multiple sites in AD brain (25, 26). Many proteases, including calpains and caspases, proteolyze Tau *in vitro* and *in vivo* (27–29). Tau can be cleaved by caspase 6 at Asp^{13} and Asp^{402}, by caspase 2 at Asp^{314}, by caspase 3 at Asp^{25} and Asp^{421}, by chymotrypsin at Tyr^{197}, by an unknown thrombin-like cytosolic protease at Lys^{257}, by asparaginyl endopeptidase at Asn^{255} and Asn^{368}, and by calpain at Lys^{44} and Arg^{230} (30–32). At Glu^{391}, Tau is cleaved by an unknown protease (30). Puromycin-specific aminopeptidase proteolyzes residues stepwise from the N terminus of Tau (4, 30). In AD brain, various Tau fragments have been identified (29, 33, 34). In addition to these protease-mediated cleavages, 21 novel proteolytic fragments of Tau have been identified (35), which, as of yet, have not had a protease identified for their generation (33, 35, 36). Among all truncations of Tau, truncations at Glu^{391} and Asp^{421} were the most reported in AD brain. We recently found that SDS- and reducing agent–resistant high-molecular-weight (HMW) aggregates of Tau from AD brain lack the N-terminal portion (21, 37). Many studies showed that truncation of Tau promotes its aggregation (30, 38), implying that Tau truncation may play a critical role in Tau pathogenesis (25, 33). However, these studies were carried out employing mostly heparin or arachidonic acid for induction of aggregation, which are highly artificial conditions. The impact of Tau truncation on its pathological activities, including hyperphosphorylation, self-aggregation, and binding to and aggregation seeded by AD O-Tau, is not well-documented. Based on the terminal acidic regions of Tau and the truncations reported in AD brain (25, 26, 39, 40), in the present study, we generated Tau truncations with deletions from both the N and C termini and determined their pathological activities. We found that Tau truncation from either the N- or C-terminal toward microtubule-binding repeat region (MTBR) modulated the site-specific phosphorylation and enhanced its self-aggregation, its binding to AD O-Tau, and aggregation seeded by AD O-Tau. Among these truncations,

‡These authors contributed equally to this work.
*For correspondence: Fei Liu, Fei.liu@opwdd.ny.gov.

© 2020 Gu et al. Published under exclusive license by The American Society for Biochemistry and Molecular Biology, Inc.

$Tau_{151–391}$ showed the highest pathological activities and aggregation induced by AD O-Tau, both *in vitro* and in cultured cells.

Results

Construction and expression of various truncation forms of Tau

In AD brain, Tau is truncated at multiple sites by various proteases (25, 33). Normally, the acidic termini of Tau interact with the microtubule-binding repeats to prevent its aggregation (41). Based on the truncation sites reported in AD brain and on the acidic terminal regions of Tau (Fig. 1*A*), we constructed 11 truncation forms of Tau from both the N and C termini of the protein (Fig. 1*A*), expressed them in HEK-293FT cells, and analyzed the expression by Western blots developed with a battery of monoclonal Tau antibodies (Fig. 1*B*). Western blots showed that the truncation forms with deletion of the first 50 amino acids (aa)—$Tau_{51–441}$, $Tau_{51–421}$, and $Tau_{51–391}$—were not recognized by antibody 43D (6–18 aa). Truncation with the deletion of the first 150 aa—$Tau_{151–441}$, $Tau_{151–421}$, and $Tau_{151–391}$—was not recognized by antibodies 43D or 63B (74–103 aa). Truncation with the deletion of the first 230 aa—$Tau_{231–441}$, $Tau_{231–421}$, and $Tau_{231–391}$—was not recognized by antibodies 43D, 63B, or Tau 5 (210–230 aa). Deletions of the last 20 aa—$Tau_{1–421}$, $Tau_{51–421}$, $Tau_{151–421}$—or the last 50 aa—$Tau_{1–391}$, $Tau_{51–391}$, $Tau_{151–391}$, and $Tau_{231–391}$—were not recognized by antibody Tau46.1 (428–441 aa) (Fig. 1*C*). mAb 77G7 against MTBR was able to detect all truncation forms (Fig. 1*C*). All truncation forms were tagged with HA at the N terminus and were detected by anti-HA (Fig. 1*C*). These results indicate that the 12 truncation forms of Tau were constructed and expressed as expected.

To learn the toxicity of these Taus, we overexpressed $Tau_{1–441}$ and 11 truncates of Tau in HEK-293T cells and analyzed lactate dehydrogenase (LDH) activity in the medium leaked from cells 48 h after transfection. We found similar levels of released LDH activity from cells overexpressed with the above 12 forms of Tau (Fig. 1*D*). We further analyzed cell viability in HEK-293T cells by Cell Counting Kit 8 and found similar cell viability in cells with overexpression of the 12 Taus (Fig. 1*D*). Thus, Tau truncates showed similar effect in cytotoxicity and cell viability as the full-length protein.

N- and C-terminal truncations modulate Tau phosphorylation

Abnormal hyperphosphorylation is central to Tau pathogenesis (3). To determine the effect of Tau truncation on its phosphorylation, we overexpressed the above truncated Taus in HEK-293FT cells and analyzed phosphorylation by Western blots developed with site-specific and phosphorylation-dependent Tau antibodies. We found no detectable Tau phosphorylation at Ser^{199}, Thr^{205}, Thr^{212}, Ser^{214}, or Thr^{217} in $Tau_{231–}$ (Fig. 2, *A–E*); at Ser^{396} or Ser^{404} in $Tau_{–391}$ (Fig. 2, *I* and *J*); and at Ser^{422} in $Tau_{–421}$ and $Tau_{–391}$ truncation forms (Fig. 2*K*), confirming the site-specific phosphorylation of Tau.

To simplify the comparison, we first analyzed the impact of N-terminal truncation on Tau phosphorylation. We found that deletion of the first 50 aa did not affect Tau phosphorylation at Ser^{199} (Fig. 2*A*), Thr^{212} (Fig. 2*C*), Ser^{214} (Fig. 2*D*), Thr^{217} (Fig. 2*E*), Ser^{235} (Fig. 2*G*), Ser^{262} (Fig. 2*H*), Ser^{396} (Fig. 2*I*), Ser^{404} (Fig. 2*J*), and Ser^{422} (Fig. 2*K*), regardless of C-terminal truncations but slightly suppressed Tau phosphorylation at Thr^{205} (Fig. 2*B*) and Thr^{231} (Fig. 2*F*). Deletion of the first 150 aa suppressed Tau phosphorylation at Ser^{199} but significantly increased it at most sites, except at Ser^{396} and Ser^{422}, independent of the C-terminal truncation (Fig. 2), suggesting that deletion of the first 150 aa enhances Tau phosphorylation at most sites. Deletion of the first 230 aa did not change ($Tau_{–441}$ and $Tau_{–421}$) or decreased ($Tau_{–391}$) Ser^{235} phosphorylation (Fig. 2*G*) but significantly increased Tau phosphorylation at Ser^{262} (Fig. 2*H*), Ser^{396} (Fig. 2*I*), Ser^{404} (Fig. 2*J*), and Ser^{422} (Fig. 2*K*) in $Tau_{–441}$ and at Ser^{262} (Fig. 2*H*) in $Tau_{–421}$ (Fig. 2*G*). However, there was no increase of Ser^{262} phosphorylation (Fig. 2*H*) in $Tau_{–391}$ and of Ser^{396} phosphorylation (Fig. 2*I*) in $Tau_{–421}$. Thus, deletion of the first 50 aa did not affect, but deletion of the first 150 aa significantly enhanced, Tau phosphorylation regardless of the C-terminal truncation. The increase in phosphorylation in Tau with deletion of the first 230 aa depended on intact or partially intact C terminus.

Then we determined the effect of the C-terminal truncations on Tau phosphorylation. We found that the C-terminal truncation also modulated Tau phosphorylation site-specifically (Fig. 3). Deletion of the last 20 aa decreased Ser^{199} phosphorylation in $Tau_{1–}$, but not in the $Tau_{51–}$ and $Tau_{151–}$ truncation forms (Fig. 3*A*). Deletion of the last 20 aa did not significantly affect Tau phosphorylation at Thr^{205}, Thr^{212}, Ser^{214}, Thr^{217}, or Ser^{262} (Fig. 3, *B–E*), increased at Ser^{235} (Fig. 3*G*), and decreased at Ser^{396} and Ser^{404} (Fig. 3, *I* and *J*) in most truncation forms. Deletion of the last 50 aa increased or tended to increase Tau phosphorylation at Thr^{205}, Thr^{212}, Ser^{214}, Thr^{217}, and Ser^{235} but did not significantly affect phosphorylation at Ser^{262} in the most N-terminal truncates (Fig. 3, *B–E*). Interestingly, deletion of the last 20 or 50 aa suppressed Ser^{262} phosphorylation in $Tau_{231–}$ truncation forms (Fig. 3*H*), and deletion of either the last 20 or 50 aa almost abolished or dramatically suppressed Tau phosphorylation at Thr^{231}, Ser^{396}, and Ser^{404} regardless of N-terminal truncation (Fig. 3, *F*, *I*, and *J*), suggesting that the last 20 aa play a critical role in the regulation of phosphorylation at these sites. These findings suggest that generally, C-terminal truncation can increase the phosphorylation of Tau at the sites located in proline-rich domain (Thr^{205}, Thr^{212}, Ser^{214}, and Thr^{217}) but decrease at sites in microtubule-binding repeat (Ser^{262}) and C-terminal domains (Ser^{396} and Ser^{404}).

Truncation of Tau promotes its aggregation

Tau is aggregated into NFTs in AD brain. To learn the impact of truncation in Tau aggregation, we overexpressed various HA-tagged truncated Taus in HEK-293FT cells for 48 h, separated RIPA buffer–soluble and –insoluble fractions, and analyzed Tau levels by Western blots developed with anti-HA. We found a significant amount of RIPA buffer–insoluble Tau in cells expressed with Tau truncations, except $Tau_{231–391}$ (Fig. 4*B*). Interestingly, we found ~70-kDa HMW-Tau only in the RIPA buffer–insoluble fraction of $Tau_{151–391}$ (Fig. 4*B*), suggesting that $Tau_{151–391}$ formed the AD-like SDS- and reducing agent–resistant aggregates described previously (21, 37).

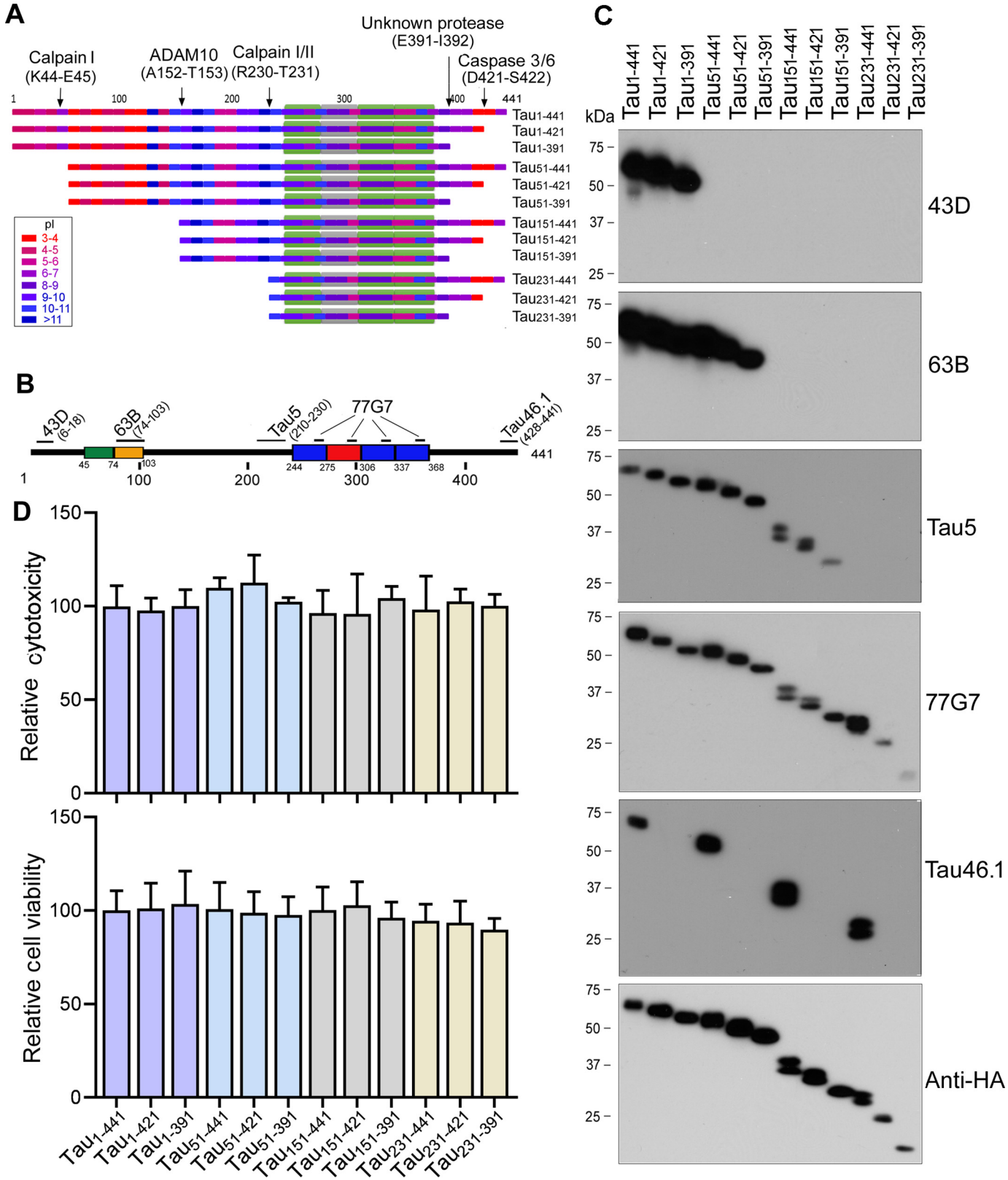

Figure 1. Truncation forms of Tau show expected size and immunolabeling in Western blots. *A*, truncation forms of Tau used in the present study. pI of every 10-aa fragment is presented with the *color code* as indicated. *B*, schematic showing the position of epitopes of Tau antibodies used in this study. *C*, truncation forms of Tau in *A* were overexpressed in HEK-293FT cells and analyzed with Western blots developed with the indicated antibodies. *D*, various truncates of Tau in *A* were overexpressed in HEK-293T cells for 48 h, and then the relative cell cytotoxicity and viability were measured by LDH activity in cultured medium and by Cell Counting Kit 8, respectively. The data are presented as means ± S.D.

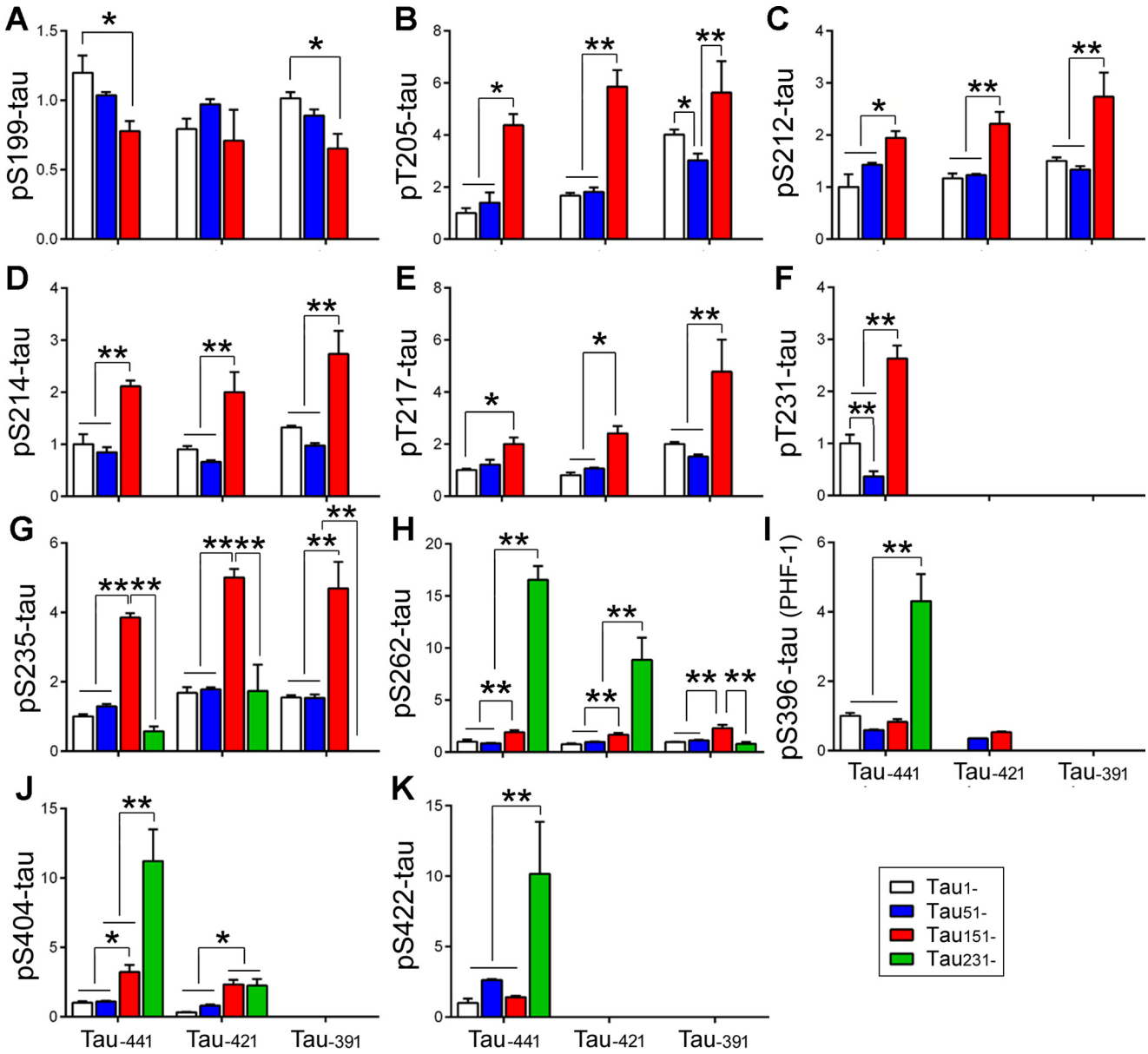

Figure 2. N-terminal truncation of Tau enhances its phosphorylation. Truncated Taus were expressed in HEK-293FT cells and analyzed by Western blots developed with site-specific and phosphorylation-dependent Tau antibodies. The phosphorylation of Tau at individual sites was calculated and statistically analyzed by one-way ANOVA. The data are presented as means ± S.D. (*A–K*). *, $p < 0.05$; **, $p < 0.01$.

We determined the impact of N-terminal truncations on Tau aggregation by analyzing the ratio of RIPA buffer–insoluble/soluble Tau. We found that in general, deletion from the N terminus toward MTBR increased the ratio of RIPA buffer–insoluble/soluble Tau (Fig. 4, *A* and *B*), suggesting that N-terminal truncation increases Tau's capacity to aggregate. Deletion of the first 50 aa did not significantly affect the ratios of RIPA buffer–insoluble/soluble Tau, regardless of the C-terminal truncations (Fig. 4, *A* and *B*). However, deletion of the first 150 aa significantly increased the ratio of RIPA buffer-insoluble/soluble Tau in Tau_{-441} and Tau_{-421}, but not in Tau_{-391} truncation forms (Fig. 4, *A* and *B*), suggesting that the first 150 aa inhibit Tau aggregation, but this inhibition depends on the intact or partially intact C terminus. Compared with Tau_{151-}, Tau_{231-} forms did not further enhance the ratios of RIPA buffer–insoluble/soluble Tau (Fig. 4, *A* and *B*), suggesting that the first 150 aa are essential to inhibit Tau self-aggregation. The expression level of $Tau_{231-391}$ was very low, which may lead to undetectable aggregation of $Tau_{231-391}$. These findings suggest that N-terminal truncation enhances Tau aggregation, and the first 150 aa are critical to prevent Tau from self-aggregation.

Deletion of C-terminal 20 aa did not affect the ratio of RIPA buffer–insoluble/soluble Tau in Tau_{1-} and Tau_{51-} but decreased in Tau_{151-} and Tau_{231-} truncation forms (Fig. 4, *A* and *C*), suggesting that the last 20 aa may not protect Tau from the self-aggregation. However, deletion of the last 50 aa significantly increased the aggregation regardless of N-terminal truncations except Tau_{231-} truncation forms (Fig. 4, *A* and *C*), suggesting that the last 50 aa are also critical to prevent Tau from self-aggregation. Taken together, these findings indicate that both the first 150 aa and the last 50 aa protect Tau from self-aggregation, and deletion of either the first 150 aa or the last 50

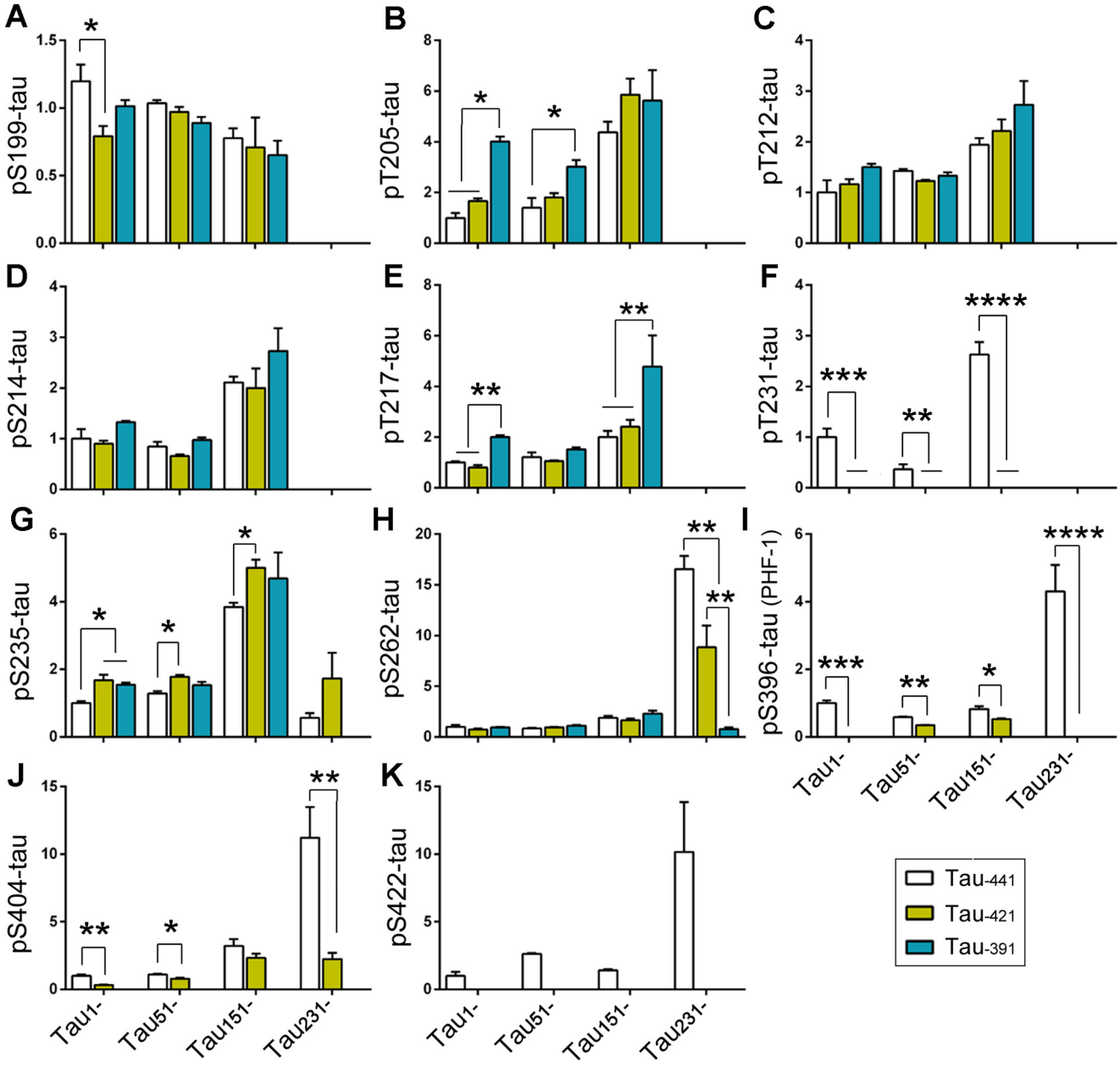

Figure 3. C-terminal truncation of Tau increases its phosphorylation at the sites in proline-rich domain and decreases at the sites in and downstream of the microtubule-binding repeats region. The phosphorylation of Tau at individual sites was normalized by total Tau and statistically analyzed by one-way ANOVA. The data are presented as means ± S.D. (*A–K*). *, $p < 0.05$; **, $p < 0.01$; ***, $p < 0.001$; ****, $p < 0.0001$.

aa promotes Tau aggregation. $Tau_{151–391}$ showed the highest self-aggregation capacity (Fig. 4).

To investigate the cause of low expression of $Tau_{231–391}$, we determined mRNA levels of Taus by real-time quantitative PCR 48 h after transfection. We found similar mRNA levels in these 12 Tau forms expressing cells (Fig. 4*E*), suggesting that a lower level of $Tau_{231–391}$ could have resulted from instability of this protein fragment.

Truncation of Tau enhances its capture by AD O-Tau

Isolated AD O-Tau was previously found to sequester/capture normal Tau (13, 14), which is a basis of Tau aggregation induced by pathological Tau. To learn the effect of Tau truncation on its capture by AD O-Tau, we performed an overlay assay. We overexpressed HA-tagged truncated Taus in HEK-293FT cells. The cell extracts containing similar levels of truncated Taus in PBS were incubated with nitrocellulose membrane predotted with various amounts of AD O-Tau overnight. AD O-Tau–captured truncated Taus were detected by development with anti-HA followed by HRP–anti-IgG and ECL. We found that Tau with various truncations was captured differentially by AD O-Tau (Fig. 5*A*). The levels of truncated Taus captured by AD O-Tau were increased with truncation from the N terminus toward MTBR (Fig. 5*A*). Deletion of the first 50 aa did not have an effect, but deletion of the first 150 aa significantly enhanced the level of Tau captured by AD O-Tau, regardless of C-terminal truncations (Fig. 5, *A* and *B*). Deletion of the first

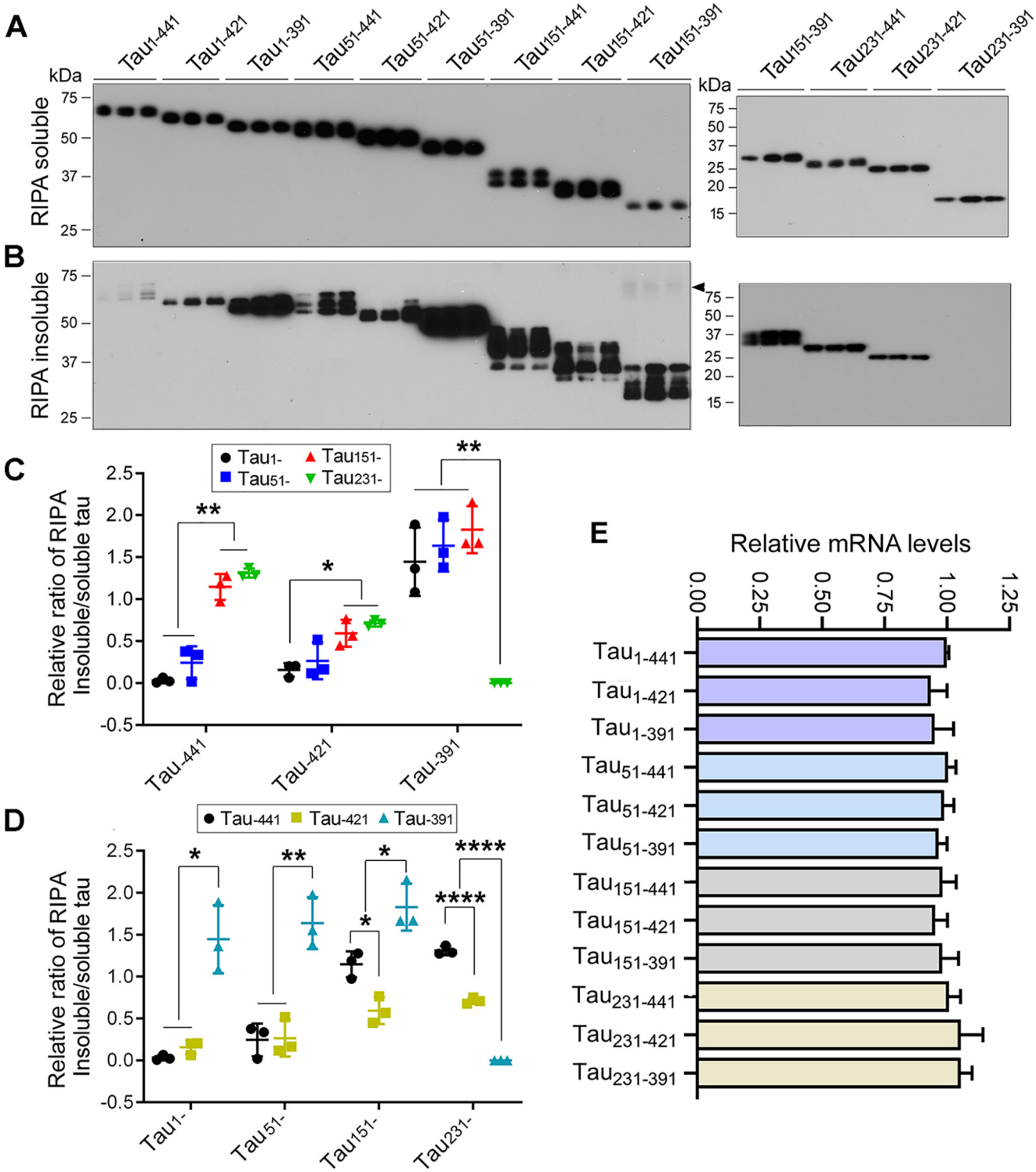

Figure 4. N- and C-terminal truncations enhance Tau's aggregation. *A* and *B*, HA-tagged truncated Taus were expressed in HEK-293FT cells for 48 h. The cells were lysed in RIPA buffer and centrifuged at 130,000 × *g* for 45 min. RIPA buffer-soluble (*A*) and -insoluble (*B*) Taus were analyzed by Western blots developed with anti-HA. The arrowhead indicates SDS- and reducing agent–resistant high molecular Tau aggregates. *C* and *D*, the ratio of RIPA buffer–insoluble/soluble Tau was calculated. The data are presented as means ± S.D. *, $p < 0.05$; **, $p < 0.01$; ****, $p < 0.0001$. *E*, various truncates of Tau were overexpressed in HEK-293T cells for 48 h. The levels of Tau mRNA were detected by quantitative RT-PCR and normalized by GAPDH. The relative levels of Tau mRNA are presented as means ± S.D.

230 aa enhanced the level of Tau captured by AD O-Tau in Tau_{-441} and Tau_{-421}, but not in Tau_{-391} truncation forms (Fig. 5, *A* and *B*). In the C-terminal truncations, deletion of the last 20 aa did not affect the capture of Tau by AD O-Tau (Fig. 5, *A* and *C*). Although deletion of the last 50 aa did not enhance Tau capture by AD O-Tau in Tau_{1-} and Tau_{51-} truncations, it enhanced it in Tau_{151-} and decreased it in Tau_{231-} forms (Fig. 5, *A* and *C*). These results suggest that the first 150 aa

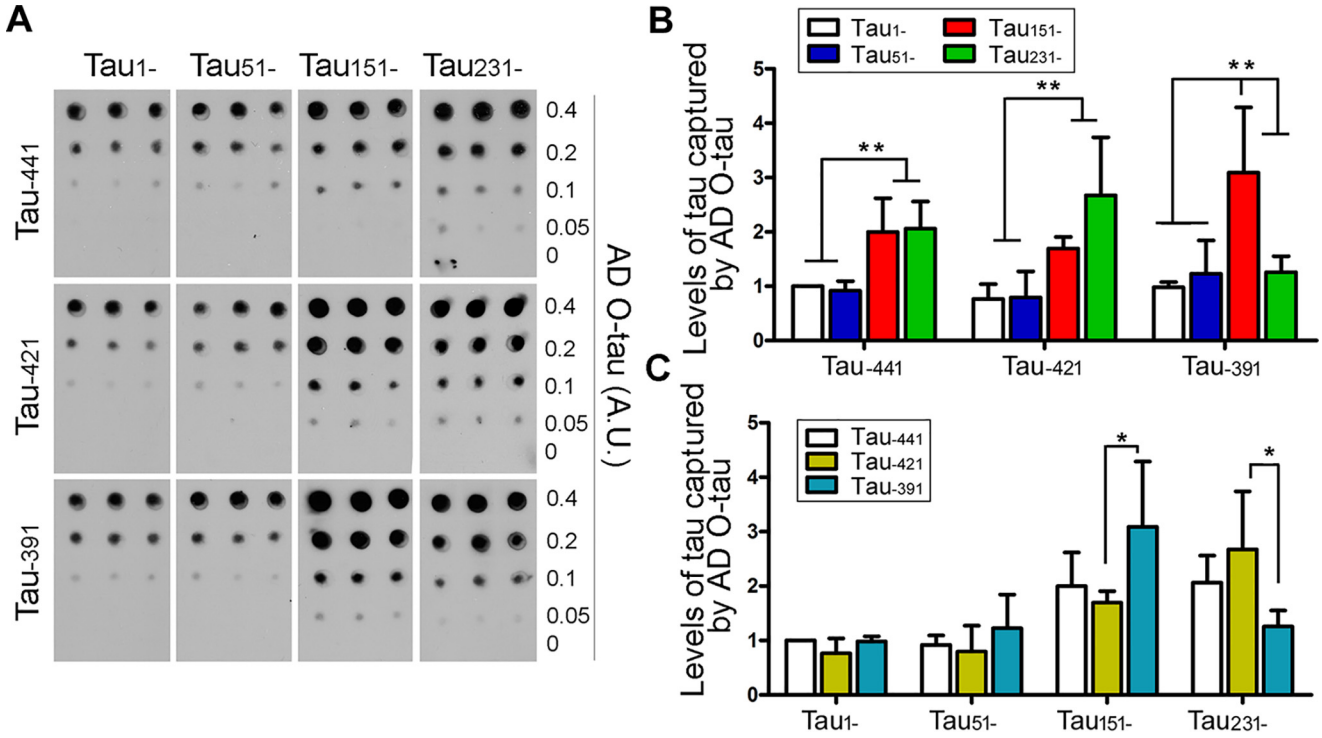

Figure 5. N- and C-terminal truncations enhance Tau's binding to AD O-Tau. HA-tagged truncated Taus were expressed in HEK-293FT cells for 48 h. The cells were lysed in PBS by probe sonication and centrifuged to yield extracts. Various amounts of AD O-Tau were dotted on nitrocellulose membrane. The membrane was incubated with cell extracts containing Tau truncations. Captured Tau was analyzed by anti-HA, followed with HRP-anti-IgG and ECL (*A*). The data are presented as means ± S.D. (*B* and *C*). *, $p < 0.05$; **, $p < 0.01$.

and the last 50 aa protect Tau from being captured by AD O-Tau, and their deletions enhance Tau's capture by AD O-Tau; $Tau_{151–391}$ is the Tau most potently captured by AD O-Tau.

Truncation of Tau enhances its aggregation seeded by AD O-Tau

Misfolded Tau templates Tau aggregation *in vitro* and *in vivo*, which is a basis of propagation of Tau pathology (14, 42). To determine the effect of Tau truncations on AD O-Tau–seeded aggregation, we overexpressed Tau truncations in HEK-293FT cells and treated these cells with AD O-Tau for 42 h after 6 h of transfection. RIPA buffer–soluble and –insoluble Taus from these cells were analyzed by Western blots. We found that the AD O-Tau treatment caused the reduction of RIPA buffer–soluble Tau (Fig. 6*A*, *upper panel*) and increased levels of RIPA buffer–insoluble Tau in all truncation forms (Fig. 6*A*, *lower panel*). In addition to the HA-Tau, AD O-Tau was detected by R134d and 92e in RIPA buffer–insoluble factions of cells treated with AD O-Tau (Fig. 6*B*). We also found HMW-Tau in the RIPA buffer–insoluble fraction of cells transfected with $Tau_{151–391}$, $Tau_{231–441}$, and $Tau_{231–421}$ (Fig. 6*A*). The expression level of $Tau_{231–391}$ was extremely low, and the RIPA buffer–insoluble Tau was undetectable in the cells treated with AD O-Tau at this condition (Fig. 6*A*). Thus, collectively these findings suggest that AD O-Tau induces Tau aggregation, which is modulated by truncation.

To compare the efficiency of aggregation of various truncated Taus seeded by AD O-Tau, we analyzed the ratio of RIPA buffer–insoluble/soluble Tau. We found that deletion of the N terminus toward MTBR increased AD O-Tau–seeded aggregation regardless of C-terminal truncation (Fig. 6, *A* and *C*). Similar to in the self-aggregation, deletion of the first 50 aa did not significantly affect Tau aggregation templated by AD O-Tau, but deletion of the first 150 aa enhanced AD O-Tau–seeded aggregation in all C-terminal truncations (Fig. 6, *A* and *C*). Deletion of the N-terminal 230 aa enhanced AD O-Tau–seeded aggregation in $Tau_{–441}$ and $Tau_{–421}$, but not in $Tau_{–391}$ truncation forms (Fig. 6, *A* and *C*). $Tau_{151–391}$ was the most potent truncation to the aggregation induced by AD O-Tau (Fig. 6, *A–D*). Deletion of the last 20 aa did not affect AD O-Tau–induced aggregation but suppressed it in $Tau_{231–}$ truncations (Fig. 6, *A* and *D*). Deletion of the last 50 aa enhanced Tau aggregation templated by AD O-Tau, except in $Tau_{231–}$ truncations (Fig. 6, *A* and *D*). These data suggest that consistently, the first 150 aa and the last 50 aa of Tau prevent AD O-Tau–seeded aggregation. Collectively, these findings reveal that deletions of either the first 150 aa or the last 50 aa can enhance AD O-Tau–seeded Tau aggregation and that $Tau_{151–391}$ is the most prone to be seeded to aggregate by AD O-Tau.

AD O-Tau induces $Tau_{151–391}$ aggregation in vitro and in cultured cells

Our studies described above indicated that $Tau_{151–391}$ appears to have the highest activity to self-aggregate and bind to AD O-Tau. Tau aggregation can be induced *in vitro* by polyanionic molecules, such as heparin, heparan sulfate, and RNA (43–45). We further studied its aggregation induced *in vitro* and in cultured cells. We first determined the aggregation of

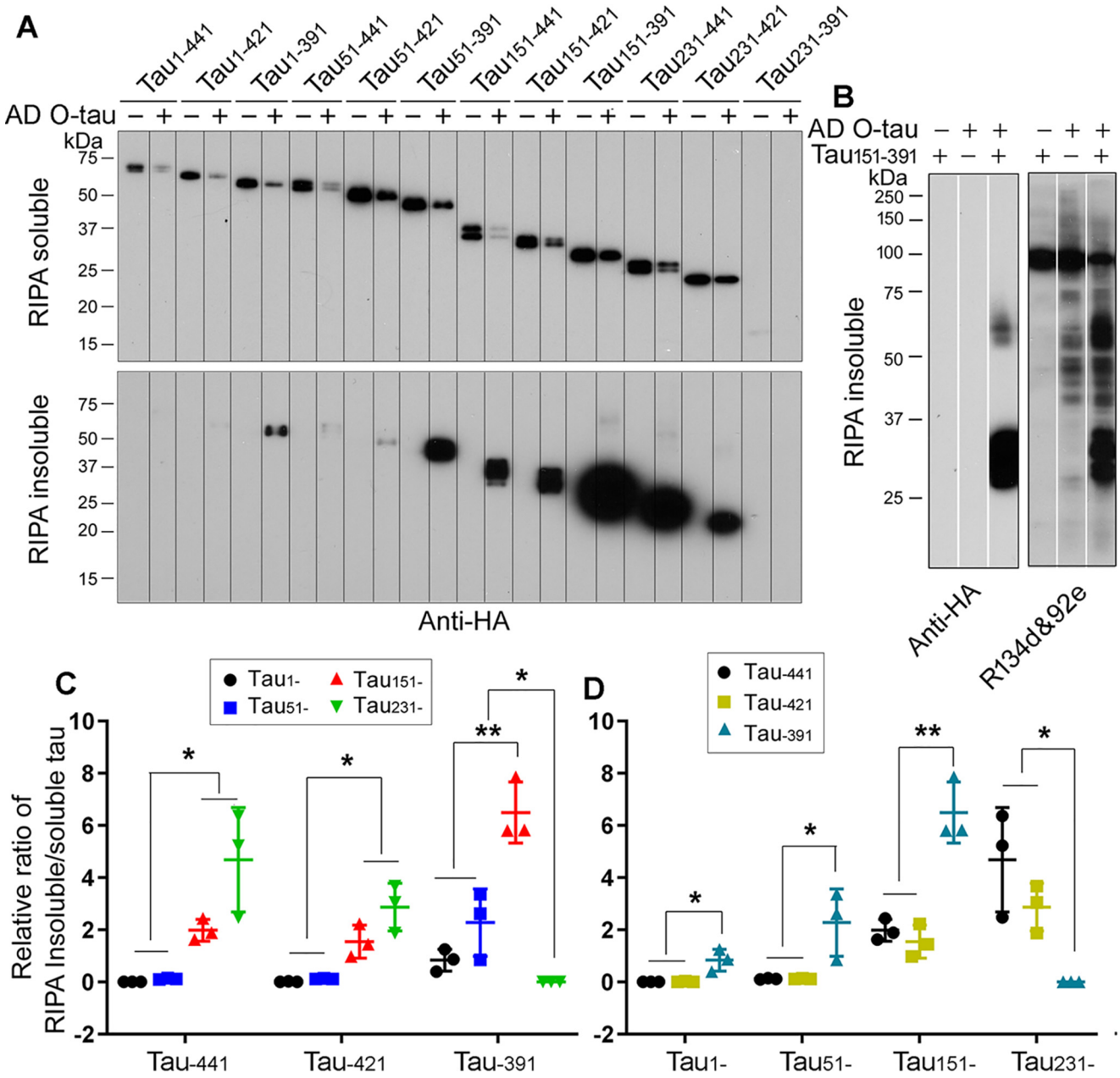

Figure 6. N- and C-terminal truncations enhance Tau aggregation seeded by AD O-Tau. *A*, HA-tagged truncated Taus were expressed in HEK-293FT cells for 6 h, and then the cells were treated with AD O-Tau for 42 h. The cells were lysed in RIPA buffer and centrifuged at 130,000 × *g* for 45 min. RIPA buffer–soluble (*upper panel*) and –insoluble (*lower p*anel) Taus were analyzed by Western blots developed with anti-HA. *B*, HA-$Tau_{151–391}$ was expressed in HEK-293FT cells. RIPA buffer–insoluble Tau was analyzed by Western blots developed with anti-HA and mixture of R134d and 92e. *C* and *D*, the ratios of RIPA buffer–insoluble/soluble Tau were calculated, and the data are presented as means ± S.D. ($n = 3$). *, $p < 0.05$; **, $p < 0.01$.

$Tau_{151–391}$ induced by heparin. We incubated recombinant $Tau_{1–441}$ ($rTau_{1–441}$) or $rTau_{151–391}$ with heparin in the presence of thioflavin T for various time periods at room temperature. Aggregated Tau was detected by fluorescence density and plotted against the incubation time. We found that heparin induced aggregation much faster and to a much higher extent in $Tau_{151–391}$ than in $Tau_{1–441}$ (Fig. 7*A*). Then we studied $Tau_{151–391}$ aggregation induced by AD O-Tau. We incubated $rTau_{151–391}$ or $rTau_{1–441}$ with AD O-Tau for various time periods at room temperature and detected aggregation by thioflavin T fluorescence. We found that AD O-Tau induced aggregation of $Tau_{151–391}$, but not $Tau_{1–441}$, in a time-dependent manner (Fig. 7*B*). These results reveal that $Tau_{151–391}$ has a higher capacity than $Tau_{1–441}$ to be induced to aggregate by either heparin or AD O-Tau *in vitro*.

To further verify AD O-Tau–induced aggregation, we overexpressed HA-tagged $Tau_{1–441}$ or $Tau_{151–391}$ in HeLa cells and treated the cells with AD O-Tau for 42 h after 6 h of transfection. The cells were then immunofluorescence-stained with anti-HA. Although we found <1% of $Tau_{1–441}$ cells with aggregates (Fig. 7, *C* and *G*), ~6% cells with atypical aggregates were seen in the $Tau_{151–391}$ cells (Fig. 7, *D* and *G*). However, we found that the treatment with AD O-Tau markedly increased the number (~22%) of $Tau_{151–391}$ cells with aggregates in the

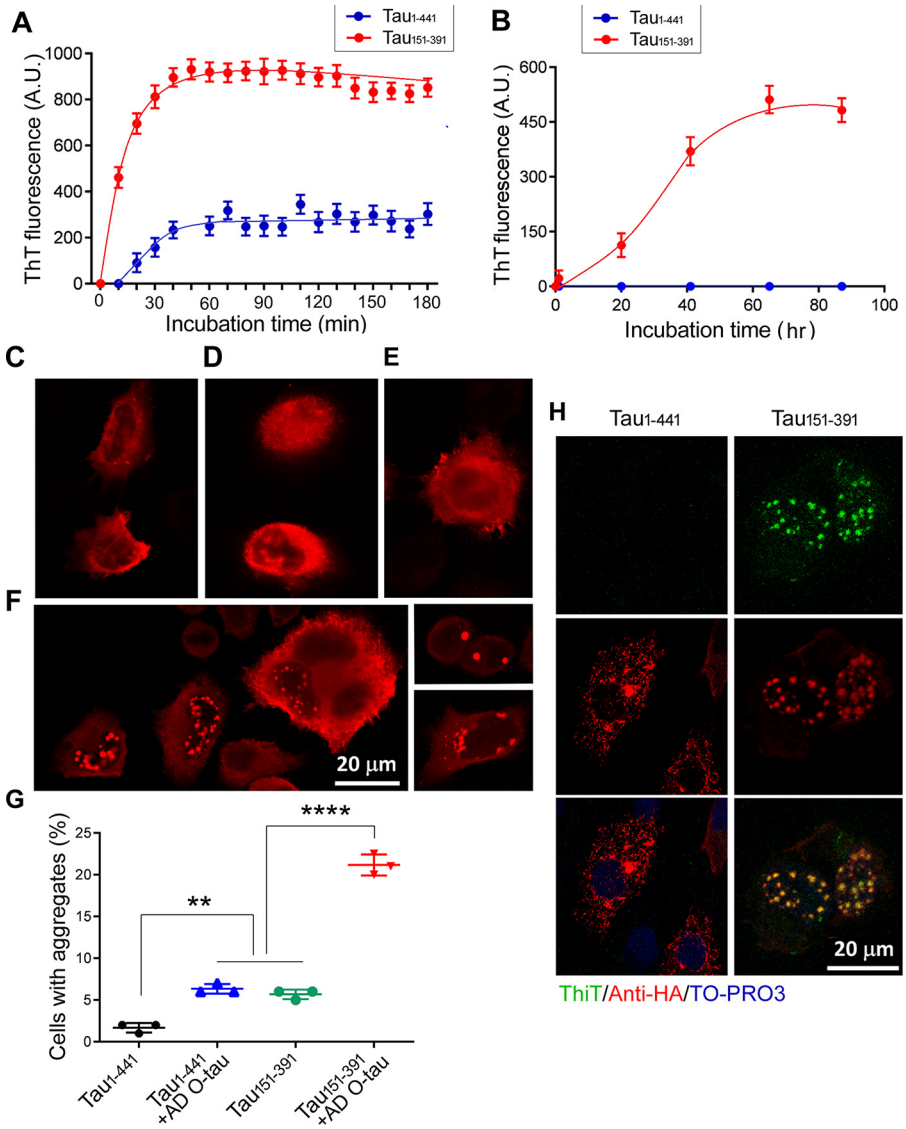

Figure 7. Aggregation of $Tau_{151–391}$ induced by AD O-Tau. *A* and *B*, recombinant $Tau_{1–441}$ and $Tau_{151–391}$ were incubated with heparin (*A*) or AD O-Tau (*B*) at room temperature for up to 180 min or 87 hr. The aggregation of Tau was measured by thioflavin T fluorescence. The data are presented as means ± S.D. (n = 3) and plotted to the incubation time. *C–F*, $Tau_{1–441}$ (*C* and *E*) and $Tau_{151–391}$ (*D* and *F*) tagged with HA were overexpressed in HeLa cells for 6 h and then treated without (*C* and *D*) or with (*E* and *F*) AD O-Tau for 42 h. The cells were immunostained with anti-HA followed by fluorescence-conjugated second antibody. *G*, the number of cells with aggregates was calculated, and the data are presented as means ± S.D. (n = 3). **, $p < 0.01$; ****, $p < 0.001$. *H*, $Tau_{151–391}$ and $Tau_{1–441}$ were overexpressed in HeLa cells and treated with AD O-Tau for 42 h. The cells were immunostained with anti-HA and co-stained with Thioflavin T.

cytoplasm and the nucleus (Fig. 7, *F* and *G*). This increase was weak in $Tau_{1–441}$ cells (Fig. 7, *E* and *G*). The aggregates of $Tau_{151–391}$, but not $Tau_{1–441}$, seeded by AD O-Tau were thioflavin T–positive (Fig. 7*H*). Thus, $Tau_{151–391}$ was found to display a high potency for templation and aggregation by AD O-Tau.

Discussion

Since the first report on Tau truncation in AD paired helical filament in 1993 (36), more than 50 fragments of Tau have been identified, and over 30 were found present in AD brain (33). However, the role of truncation in Tau pathogenesis in AD and related tauopathies was not well-understood. Based on several reported cleavage sites, in the present study we studied effects of different Tau truncations on pathological activities. We found that truncation at both the N and C termini enhanced pathological activities of Tau, including an increase of site-specific hyperphosphorylation, self-aggregation, capture by AD O-Tau, and AD O-Tau–seeded aggregation (Fig. 8). Among the truncated fragments, $Tau_{151–391}$ was found to be the most pathogenic.

Prion-like activity of pathological Tau may underlie the progression of AD and related tauopathies. Our group previously found that recombinant Tau can be sequestered by AD P-Tau by overlay assay (13). In the present study, we developed a novel assay with AD O-Tau as capture to quantitively validate the ability of Tau "seeds" to capture pro-aggregation truncated Tau fragments, which is a significant advance over artificial conditions using heparan or other methods to induce aggregation.

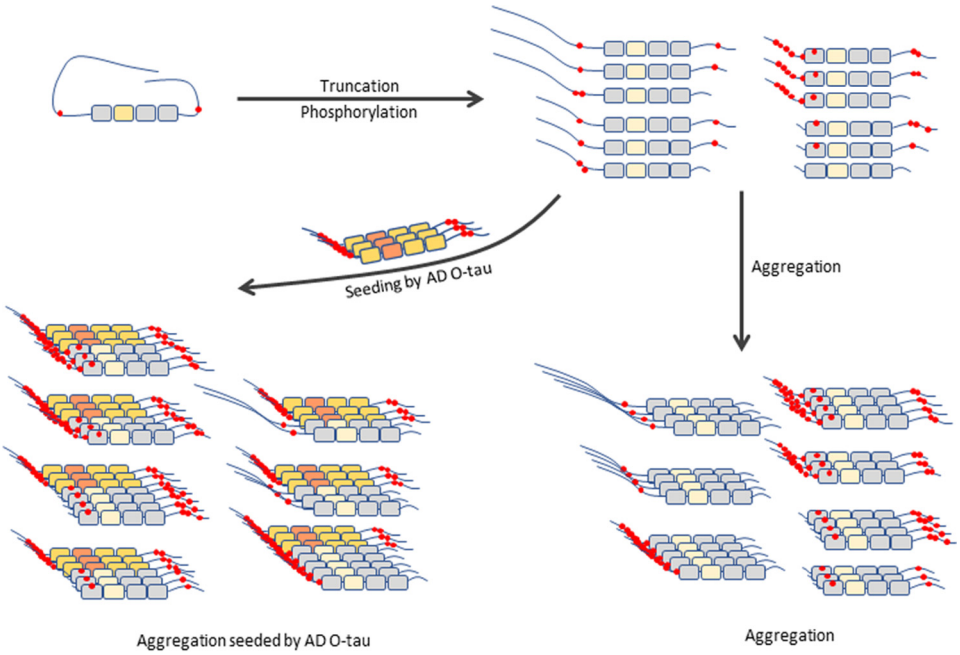

Figure 8. Proposed Tau truncation and its pathological activities. Deletion of the first 150 aa and the last 50 aa enhances Tau hyperphosphorylation, aggregation, and binding to and aggregation seeded by AD O-Tau. $Tau_{151–391}$ is prone to aggregation.

Here we found that N-terminal truncation is particularly significant to pathogenesis, whereas prior work focused on C-terminal truncation. Our present study also challenges the dogma of the importance of caspase cleavage at Asp^{421} because we did not find any increase in pathogenic activity in Tau truncated at this site. The capture assay identified pathological cores for assembly, which mimic the early steps of Tau aggregation. Similarly, the method also can be used to detect prion-like activity of pathological Tau by overlay with crude extract of HEK-293FT/HA-$Tau_{151–391}$.

Tau RD P301S FRET Biosensor, in which a HEK-293 cell line that stably expresses the repeat domain (amino acids 244–372) of 2N4R Tau with two disease-associated mutations (P301L and V337M), is widely used to assess prion-like seeding activity (46). We here expressed various forms of HA-Tau in HEK-293FT cells, treated the cells with AD O-Tau for 42 h after 6 h transfection, and harvested the cells with RIPA buffer. Aggregated Tau induced by AD O-Tau was yielded in RIPA buffer–insoluble fraction by 130,000 × *g* for 45 min and quantified by immunoblots. By using this method, we found different efficacies of various Tau truncates in AD O-Tau seeded aggregation in cultured cells, and $Tau_{151–391}$ was found to be the most prone to be induced to aggregate. Consistently, we found that N-terminal truncation is more significant to pathogenesis than C-terminal truncation at Asp^{421}. This method also can be used to evaluate the seeding activity of pathological Tau from AD and 3xTg-AD mouse brains (21).

Heparin and other polyanionic molecules had been shown to induce Tau aggregation *in vitro* (44, 45, 47). Therefore, heparin-induced Tau aggregation assay combined with thioflavin T fluorescence detection was most commonly used to access Tau aggregation (48, 49). Nevertheless, heparin-induced filament core is structurally different from that seen in the AD brain (49). In this study, $Tau_{151–391}$ aggregation *in vitro* was induced by incubating with AD O-Tau. However, the prion-like activity of AD O-Tau–induced Tau aggregates *in vivo* remains to be investigated.

Tau molecule shows a preference to form a paperclip-like conformation by folding the acidic N- and C-terminal portions back on the basic MTBR region (50) (Fig. 8), which might protect Tau from self-aggregation. It was reported that two sequences, ^{275}VQIINK^{280} and ^{306}VQIVYK^{311}, within repeats (R) 1 and 2, respectively, of the MTBR are required for self-aggregation of Tau protein (51, 52). In the present study, we found that deletion of either the first 50 aa or the last 20 aa, which removes part of the acidic N and C termini, did not significantly affect Tau's self-aggregation and its binding to and aggregation seeded by AD O-Tau. However, deletion of either the first 150 aa or the last 50 aa, which removes the acidic portions of N or C terminus completely, markedly increased the pathological activities of Tau (Fig. 8). Thus, both the N- and C-terminal acidic portions of Tau appear to protect Tau from aggregation. Partial deletion of the N- or C-terminal acidic regions may not be able to disrupt the paperclip structure, but complete removal of these acidic regions probably disrupts the paperclip structure and increases the aggregation tendency. Thus, $Tau_{151–391}$ is the most prone to (*a*) self-aggregation, (*b*) binding to AD O-Tau, and (*c*) AD O-Tau–seeded aggregation. Interestingly, deletion of 230 aa increased self-aggregation, its capture by AD O-Tau, and AD O-Tau-seeded aggregation in Tau_{-441} and Tau_{-421} truncation forms as compared with deletion of the first 150 aa. However, Although $Tau_{231–391}$ was captured by AD O-Tau efficiently, no self-aggregation and AD O-Tau–induced aggregation of Tau were detected in $Tau_{231–391}$ cells. We found a very low expression level of $Tau_{231–391}$ in cells, which could be a reason why we could not find any detectable Tau aggregation with or without AD O-Tau induction. However, mRNA level of $Tau_{231–391}$ was similar to

other Tau truncates in cells, suggesting a lower stability of the protein.

Aggregation of hyperphosphorylated Tau into NFTs is apparently central to the pathogenesis of AD and related tauopathies (3). In AD brain, Tau is hyperphosphorylated and truncated. Caspase cleavage of Tau may precede the hyperphosphorylation, where especially caspase cleavage at Asp^{421} has been shown to initiate the cascade leading to Tau aggregation (29, 53, 54). In the present study, we found that deletion of the first 50 aa did not affect significantly Tau phosphorylation. However, deletion of the first 150 aa increased Tau phosphorylation at Thr^{205}, Thr^{212}, Ser^{214}, Thr^{217}, Thr^{231}, and Ser^{235}, but not at Ser^{262}, Ser^{396}, Ser^{404}, and Ser^{422}, suggesting that deletion of the 150 aa makes the region upstream of MTBR, but not MTBR and downstream of MTBR, a favorable substrate for Tau kinases and/or an unfavorable substrate for Tau phosphatases. It is also possible that facilitation of Tau phosphorylation by the truncation may result from the molecule opening or/and from reduction of acidic nature of the molecule by deletion of the N-terminal portion. Similarly, deletion of N-terminal 230 aa enhanced Tau phosphorylation at the sites in MTBR and downstream of it. However, deletion of C-terminal either 20 aa or 50 aa did not increase or weakly increased Tau phosphorylation at the majority of phospho-sites but suppressed that at Thr^{231}, Ser^{262}, Ser^{396}, and Ser^{404}. Thus, N-terminal truncation generally enhanced, but C-terminal truncation suppressed, Tau phosphorylation. Hyperphosphorylation leads to Tau aggregation (55). Pseudo-phosphorylation at Ser^{396} and Ser^{404} stimulates the rate of Tau polymerization (56). Thus, truncation at the N terminus may also enhance Tau aggregation via hyperphosphorylation.

Many proteases are expressed in the infant brain, including A disintegrin and metalloproteinase 10 (ADAM10), thrombin, caspase, and calpain. Under physiological circumstances, they are involved in the control of brain development via regulating multiple substrates in the signal cascades, brain inflammation, apoptosis, and so on. In AD, up-regulation and/or mislocalization of these proteases could lead to increased levels and/or inappropriate positioning of truncated Tau. Unlike in infant or normal adult brain, in AD brain hyperphosphorylation probably opens Tau's paper clip structure, which makes its cleavage at aa 150 by thrombin and/or ADAM 10 possible (57). Furthermore, an elevated level of Tau in AD brain provides abundant substrate for the proteases and aggravates the pathological accumulation of truncated fragments.

Two proteases, thrombin and ADAM10, which cleave Tau at Arg^{155} and Ala^{152}, respectively, might be responsible for N-terminal truncation of Tau near Lys^{150} *in vivo* (33, 58, 59). Both enzymes are expressed in adult human brain (58, 60). ADAM10, first identified as the primary α-secretase of β-amyloid protein precursor (61), showed a 2-fold increase of mRNA levels in AD hippocampus (62). It is mainly localized to cell membrane and functions as a transmembrane protease, but its activity may not be limited to the membrane. For example, ADAM10 might exert proteolytic activity in its trafficking route to the plasma membrane, and ADAM10 still functions at the early stages after endocytosis when it is not fully degraded (63, 64). Although Tau is mostly cytoplasmic, it is released in the extracellular space through multiple pathways including direct leakage, exocytosis, exosomes, synaptic vesicles, or translocation across the plasma membrane (65). In addition, we cannot exclude the possibility that Tau might be cleaved extracellularly and then internalized. It was reported that ADAM10-cleaved Tau fragment (Tau-A) was elevated 10-fold high in the brains of the Tg4510 mouse model of Tau deposition (66). Although high levels of serum Tau-A were associated with lower risk of AD and dementia in a prospective study (67), serum Tau-A levels did show a significant increase in AD and mild cognitive impairment (68). In AD patients, Tau-A level in serum correlated inversely with the cognitive assessment score (Mattis dementia rating scale) (65) and was related to the change of cognitive function over time in early AD patients (69), supporting the possibility that Tau-A could indicate the rate of clinical progression of AD. Thrombin stains extra- and intracellular NFTs, implying that the enzyme could function both outside and inside cells (58). Nevertheless, the current evidence is not sufficient to reveal whether ADAM10 and thrombin cleave Tau intracellularly or extracellularly or both.

NFTs in AD contains full-length Tau (70). The truncations probably occur after NFTs are formed and after cell death become extracellular. However, we recently reported that HMW-Tau in AD brains lacked the N-terminal portion (37). The truncations could play a significant role as aggregation-promoting seeds and thus in this way become important in promoting and accelerating secondary spread of Tau pathology. Thus, it remains to be investigated whether these truncations occur prior to aggregation of Tau in one or more tauopathies other than AD.

Truncations of Tau at Asp^{421} (Tau_{D421}) and Glu^{391} (Tau_{E391}) are the most studied truncation forms in AD brain. Tau is cleaved at Asp^{421} by caspase-3 and at Glu^{391} by an unknown protease. Tau_{D421} and Tau_{E391} aggregate more rapidly and to a greater degree than full-length Tau in the presence of heparin or arachidonic acid (38, 56). Tau_{D421} and Tau_{E391} detected by the mAb C3 and mAb423 are also present at early stages of Tau aggregation (71, 72). Immunohistochemical studies indicate that cleavage at Asp^{421} occurs after formation of the Alz50 epitope but prior to truncation at Glu^{391}. Thus, Tau_{D421} appears to occur relatively early in the disease state, contemporaneous with the initial Alz50 folding event that heralds the appearance of filamentous Tau in NFTs, neuropil threads, and the dystrophic neurites surrounding amyloid plaques (73). The levels of Tau fragment cleaved at Asp^{421} (Tau-C) in serum were not significantly related to the change of cognitive function over time in early AD patients (69). In AD brain, the level of Tau_{D421} is increased significantly (29, 74, 75) but was not found in HMW-Tau (37). In the present study, we found that truncation of Tau at Asp^{421}, a partial deletion of the acidic C-terminal, did not enhance the self-aggregation in cultured cells and AD O-Tau–seeded aggregation in cultured cells, which may be due to the reduction of Tau phosphorylation at Thr^{231}, Ser^{262}, Ser^{396}, and Ser^{404}. In a previous study we showed that hyperphosphorylation of Tau at Thr^{231} and Ser^{262} are required for its self-aggregation into paired helical filaments (PHFs) *in vitro* (76). In contrast to Tau_{D421} and Tau_{E391}, the deletion of the whole acidic C-terminal region dramatically enhanced Tau self-aggregation,

ASBMB

capture by AD O-Tau, and AD O-Tau–seeded aggregation. Further deletion of N-terminal 150 aa, which results in $Tau_{151–391}$, the Tau fragment of the protease-resistant core of PHFs isolated from AD brain (77), showed the highest pathological activities. Rats transgenic for $Tau_{151–391}$ develop neurofibrillary pathology and also display hyperphosphorylation and production of HMW-Tau species (25). In addition, SDS- and β-mercaptoethanol–resistant HMW-Tau in AD brain homogenates was immunoreactive with anti–$pSer^{422}$-Tau strongly. Thus, these findings argue against the impact of Tau truncation at Asp^{421} in Tau pathogenesis and suggest that N-terminal truncation is particularly significant to pathogenesis of AD.

Our previous studies showed that hyperphosphorylation of Tau inhibits its binding to tubulin and promotion of the assembly and stabilization of microtubules and increases its self-aggregation and its capture of normal Tau, the characteristics that suggest the opening of the paperclip structure of Tau (13–15). The present study suggests that truncation of Tau generating $Tau_{151–391}$ results in similar characteristics. Furthermore, truncation of Tau at Lys^{150} enhances Tau phosphorylation. Thus, in addition to the inhibition of the hyperphosphorylation, inhibition of the proteases responsible for the truncation of Tau at Lys^{150} and/or Glu^{391} could be required to effectively inhibit Tau pathology.

Although similar cytotoxicity and cell viability were found in cells overexpressing various Tau truncates, truncation may generate toxic Tau fragments. N-terminal Tau fragments including Tau 1–44 aa, 26–44 aa, 26–230 aa, 1–156 aa, and 45–230 aa exert powerful toxicity (78–80), but Tau 1–230 aa protects neuron from apoptosis (78). Activation of calpain by aggregated Aβ generated a neurotoxic 17-kDa fragment (81, 82). Deletion of the microtubule-binding domain facilitates the spine localization of Tau (82). Phosphorylation of Tau at distinct sites increases Tau targeting spine, which may regulate the spine localization of Src kinase Fyn (82, 83). Thus, truncation of Tau may have broad roles in AD pathogenesis.

We analyzed here Tau truncation and its pathological changes *in vitro* and in cultured HEK-293FT cells that do not contain high concentration of assembled microtubules or axonal processes. Also, unique Tau kinase-sensitive phosphorylated sites and chaperones like HSP90 influence normal folding and what is exposed to proteases. Thus, the role of Tau truncation and its phosphorylation, interaction with, and aggregation seeded by AD O-Tau remain to be studied in neuronal cells and *in vivo*.

In summary, the acidic N and C termini of Tau suppress its pathological activities. Truncation of Tau from the N or C terminus toward MTBR enhances its site-specific phosphorylation, self-aggregation, capture by AD O-Tau, and AD O-Tau–seeded aggregation. Deletion of either the first 150 aa or the last 50 aa, but not the first 50 aa or the last 20 aa, markedly increases the pathological activities, which may initiate Tau pathogenesis in AD brain and related tauopathies. $Tau_{151–391}$ is the most potent Tau fragment for pathological activities, which can be used for seeding activity *in vitro* and *in vivo*. Inhibition of Tau truncation may be a therapeutic approach to prevent or inhibit Tau pathogenesis.

Materials and methods

Plasmids, antibodies, and other reagents

pCI/HA-Tau truncations were generated by PCR amplification with the primers listed in Table 1 by using pCI/HA-Tau as a template and were constructed into pCI-neo. All constructs were verified by DNA sequence analysis. The primary antibodies used in the present study are listed in Table 2. Peroxidase-conjugated anti-mouse and anti-rabbit IgGs were obtained from Jackson ImmunoResearch Laboratories (West Grove, PA). Alexa Fluor 555–conjugated goat anti-mouse IgG was from Life Technologies Inc. Heparin and thioflavin T were from Sigma–Aldrich. CyQUANT™ LDH cytotoxicity assay kit and the ECL kit were from Thermo Fisher Scientific. Cell Counting Kit 8 was from Dojindo Molecular Technologies (Rockville, MD).

Cell culture and transfection

HEK-293FT, HEK-293T, and HeLa cells were maintained in Dulbecco's modified Eagle's medium supplemented with 10% fetal bovine serum (Thermo Fisher Scientific) at 37 °C (5% CO_2). Transfections were performed with FuGENE HD (Promega, Madison, WI) according to the manufacturer's instructions.

Western blots and immunodot blots

The samples were diluted with Laemmli SDS sample buffer, followed by boiling for 5 min. Protein concentration was measured using the Pierce™ 660-nm protein assay kit (Thermo Fisher Scientific). The samples were subjected to SDS-PAGE and transferred onto polyvinylidene fluoride membrane (Sigma-Aldrich). The membrane was subsequently blocked with 5% fat-free milk–TBS for 30 min, incubated with primary antibodies (Table 2) in TBS overnight, washed with TBST (TBS with 0.05% Tween 20), incubated with HRP-conjugated secondary antibody for 2 h at room temperature, washed with TBST, incubated with the ECL Western blotting substrate (Thermo Fisher Scientific), and exposed to HyBlot CL® autoradiography film (Denville Scientific Inc., Holliston, MA). Specific immunostaining was quantified by using the Multi Gauge software V3.0 from Fuji Film (Minato, Tokyo, Japan).

Tau level in samples was assayed by immunodot blots as described previously. Briefly, various amounts of a sample were applied onto nitrocellulose membrane (Schleicher and Schuell, Keene, NH) at 5 μl/grid of 7 × 7 mm. The blot was placed in a 37 °C oven for 1 h to allow the protein to bind to the membrane. The membrane was processed as Western blots as described above by using the mixture of R134d and 92e pan Tau antibodies as primary antibodies.

Cytotoxicity and viability assay

Cell cytotoxicity was assessed by measuring LDH release from damaged or dead cells using a CyQUANT LDH cytotoxicity assay kit (Thermo Fisher Scientific) following the manufacturer's instructions. Briefly, HEK-293T cells in 96-well plate were transfected with pCI/HA-Taus with FuGENE HD for 48 h. The culture mediums were collected and incubated with the

Table 1
Primers used in this study

Truncations	Primer	
	Forward	Reverse
Tau_{1-441} (SalI, NotI)	ACGCGTCGACATGTACCCATACGATGTTCCAGATTACGCTatggctgagccccgcaggagttcg	ataagaatgcggccgctcacaaaccctgcttggcccagggagg
Tau_{1-421} (SalI, NotI)	ACGCGTCGACATGTACCCATACGATGTTCCAGATTACGCTatggctgagccccgcaggagttcg	ataagaat gcggccgctcactccgccccgtggtctgtcttgg
Tau_{1-391} (SalI, NotI)	ACGCGTCGACATGTACCCATACGATGTTCCAGATTACGCTatggctgagccccgcaggagttcg	ataagaatgcggccgctcaGTCtaccatgtcgatgctgccgg
Tau_{51-441} (SalI, NotI)	ACGCGTCGACATGTACCCATACGATGTTCCAGATTACGCTATGaccccactgaggacggatctga	ataagaatgcggccgctcacaaaccctgcttggcccagggagg
Tau_{51-421} (SalI, NotI)	ACGCGTCGACATGTACCCATACGATGTTCCAGATTACGCTATGaccccactgaggacggatctga	ataagaat gcggccgctcactccgccccgtggtctgtcttgg
Tau_{51-391} (SalI, NotI)	ACGCGTCGACATGTACCCATACGATGTTCCAGATTACGCTATGaccccactgaggacggatctga	ataagaatgcggccgctcaGTCtaccatgtcgatgctgccgg
$Tau_{151-441}$ (SalI, NotI)	ACGCGTCGACATGTACCCATACGATGTTCCAGATTACGCTatgccacaccgcggggagcag	ataagaatgcggccgctcacaaaccctgcttggcccagggagg
$Tau_{151-421}$ (SalI, NotI)	ACGCGTCGACATGTACCCATACGATGTTCCAGATTACGCTatgccacaccgcggggagcag	ataagaat gcggccgctcactccgccccgtggtctgtcttgg
$Tau_{151-391}$ (SalI, NotI)	ACGCGTCGACATGTACCCATACGATGTTCCAGATTACGCTatgccacaccgcggggagcag	ataagaatgcggccgctcaGTCtaccatgtcgatgctgccgg
$Tau_{231-441}$ (SalI, NotI)	ACGCGTCGACATGTACCCATACGATGTTCCAGATTACGCTATGactccaccaagtcgccgtcttccgc	ataagaatgcggccgctcacaaaccctgcttggcccagggagg
$Tau_{231-421}$ (SalI, NotI)	ACGCGTCGACATGTACCCATACGATGTTCCAGATTACGCTATGactccaccaagtcgccgtcttccgc	ataagaatgcggccgctcactccgccccgtggtctgtcttgg
$Tau_{231-391}$ (SalI, NotI)	ACGCGTCGACATGTACCCATACGATGTTCCAGATTACGCTATGactccaccaagtcgccgtcttccgc	ataagaatgcggccgctcaGTCtaccatgtcgatgctgccgg

reaction mixture for 30 min at room temperature. Maximum was yielded by adding lysis buffer to release all LDH to medium. The A_{490} and A_{680} were recorded by universal microplate spectrophotometer (BioTek, Winooski, VT) after adding stop solution. Relative cytotoxicity to Tau_{1-441} was calculated according to the formulas in the manufacturer's instructions.

For cell viability assay, HEK-293T cells cultured in 96-well were transfected with pCI/HA-Taus for 48 h. After adding 10 μl of Cell Counting Kit 8 to each well and incubating at 37 °C for 1 h, A_{450} was recorded, and relative cell viability to Tau_{1-441} was calculated.

Quantitative RT-PCR

Total RNA was extracted from cells by using the HP total RNA kit (Omega Bio-tek, Norcross, GA) according to the manufacturer's instructions. Equal amount of RNA was reverse transcribed to cDNA by using SuperScript first-strand cDNA synthesis kit (Biouniquer, Nanjing, China). Real-time PCR was performed with AceQ® quantitative PCR SYBR® Green Master Mix (without ROX) kit (Vazyme Biotech, Nanjing, China) on a LightCycler® 96 real-time PCR system (Roche Diagnostics). The PCR conditions were as follows: 95 °C for 10 min; followed by 45 cycles of 95 °C for 10 s and 60 °C for 30 s; and then 95 °C for 10 s; 65 °C for 60 s; 97 °C for 1 s; and 37 °C for 30 s. The quantitative PCR was performed using these primers: human Tau (forward, 5′-CCAAGTGTGGCTCATTAGGCA-3′; reverse, 5′-CCAATCTTCGACTGGACTCTGT-3′), human GAPDH (forward, 5′-CATGAGAAGTATGACAACAGCCT-3′; reverse, 5′-AGTCCTTCCACGATACCAAAGT-3′). Relative levels of mRNA were quantified by the comparative $2^{-\triangle\triangle CT}$ method and normalized to GAPDH level.

Preparation of hyperphosphorylated and AD O-Tau

AD O-Tau was isolated from the cerebral cortex of frozen autopsied AD brains as we described previously (10). Briefly, 10% brain homogenate prepared in buffer (20 mM Tris-HCl, pH 8.0, 0.32 M sucrose, 10 mM β-mercaptoethanol, 5 mM $MgSO_4$, 1 mM EDTA, 10 mM glycerophosphate, 1 mM Na_3VO_4, 50 mM NaF, 1 mM 4-(2-aminoethyl) benzenesulfonyl fluoride hydrochloride (AEBSF), and 10 mg/ml each of aprotinin, leupeptin, and pepstatin) was centrifuged at 27,000 × *g* for 30 min. The supernatant was further centrifuged at 235,000 × *g* for 45 min, and the resulting pellet, *i.e.* AD O-Tau–enriched fractions, was collected, washed three times, and then resuspended in normal saline. The AD O-Tau was probe-sonicated for 10 min at 20% power and stored at −80 °C.

Tau captured by AD O-Tau assay

Various Tau truncations tagged with HA at the N terminus were overexpressed in HEK-293FT cells for 48 h. The cells were lysed in PBS containing 50 mM NaF, 1 mM Na_3VO_4, 1 mM AEBSF, 5 mM benzamidine, and 10 μg/ml each of aprotinin, leupeptin, and pepstatin by probe sonication at 20% power for 2 min. The cell lysates were centrifuged for 10 min at 10,000 × *g*. The supernatants containing HA-Tau truncations were stored at −80°C until used.

ASBMB

Table 2
Primary antibodies used in the present study
Mono, monoclonal; Up, unphosphorylated; Poly, polyclonal; M, mouse; R, rabbit.

Antibody	Type	Species	Specificity	Source/reference (catalog or lot no.)
43D	Mono	M	$Tau_{8–16}$	BioLegend (816601) (21)
63B	Mono	M	$Tau_{74–103}$	In house (21)
TAU5	Mono	M	$Tau_{210–241}$	Millipore (MAB361/1816394)
77G7	Mono	M	$Tau_{316–355}$	BioLegend (816701) (21)
Tau46.1	Mono	M	$Tau_{428–441}$	Upstate (05-838/27088)
R134d	Poly	R	Total Tau	In house (21)
Anti-pS199	Poly	R	$pSer^{199}$	Invitrogen (44-734G/0300A)
Anti-pT205	Poly	R	$pThr^{205}$	Invitrogen (44-738G/RD214239)
Anti-pT212	Poly	R	$pThr^{212}$	Invitrogen (44-740G/1709582A)
Anti-pS214	Poly	R	$pSer^{214}$	Invitrogen (44-742G/0500B)
Anti-pT217	Poly	R	$pSer^{217}$	Invitrogen (44-744/785771A)
AT180	Mono	M	$pThr^{231}$	Invitrogen (MN1040/SH2406086)
Anti-pS235	Poly	R	$pSer^{235}$	BIOSOURCE (22-3490-0)
Anti-pS262	Poly	R	$pSer^{262}$	Invitrogen (44-750G/QK220618)
Anti-pS396	Poly	R	$pSer^{396}$	Invitrogen (44752G/567847B)
Anti-pS404	Poly	R	$pSer^{404}$	Invitrogen (44-758G/5G255476)
R145d	Poly	R	$pSer^{422}$	In house (84)
PHF-1	Mono	M	$pSer^{396}$	Dr. Peter Davies
92e	Poly	R	Total Tau	In house (21)
Anti-HA	Mono	M	HA	Sigma (H9658/101M4776)
Anti-HA	Poly	R	HA	Sigma (H6908/110M4845)
Anti-GAPDH	Poly	R	GAPDH	Sigma (G9545/015M4824V)
Anti–β-actin	Mono	M	β-Actin	Sigma (A1978/046M4789V)

Various amounts of AD O-Tau isolated from AD brains were dotted on nitrocellulose membrane after serial dilution in TBS and dried at 37 °C for 1 h. The membrane was blocked with 5% fat-free milk in TBS for 2 h and incubated with the above cell extracts containing HA-tagged truncated Taus overnight. After washing three times with TBST, the membrane was incubated with anti-HA in 5% milk in TBST overnight and processed as immuno-dot blot as described above.

AD O-Tau seeded Tau aggregation in cultured cells

HEK-293FT cells were transfected with pCI/HA-Tau truncations with FuGENE HD. AD O-Tau from AD brains was mixed with Lipofectamine 2000 (3.0% in Opti-MEM) (Thermo Fisher Scientific) in 50 μl for 20 min at room temperature. The AD O-Tau/Lipofectamine was added into the cell cultures in 24-well plates after 6 h of transfection and cultured for 42 h. The cells were lysed in RIPA buffer (50 mM Tris-HCl, 150 mM NaCl, 1% Nonidet P-40, 0.5% sodium deoxycholate, and 0.1% SDS) containing 50 mM NaF, 1 mM Na_3VO_4, 1 mM AEBSF, 5 mM benzamidine, and 10 μg/ml each of aprotinin, leupeptin, and pepstatin for 20 min on ice. The cell lysates were centrifuged at 130,000 × *g* for 45 min, and the resulting pellet was washed twice with RIPA buffer. The supernatants were pooled together as RIPA buffer–soluble fraction, and the pellet was the RIPA buffer–insoluble fraction. Levels of RIPA buffer–insoluble and -soluble Tau were analyzed by Western blots developed with anti-HA.

To visualize the Tau aggregates in cells, HeLa cells were overexpressed with $Tau_{1–441}$ and $Tau_{151–391}$ tagged with HA and treated with AD O-Tau for 42 h as described above. The cells were then fixed for 15 min with 4% paraformaldehyde in phosphate buffer, washed with PBS, and treated with 0.3% Triton in PBS for 15 min at room temperature. After blocking with 5% newborn goat serum, 0.1% Triton X-100, and 0.05% Tween 20 in PBS for 30 min, the cells were incubated with anti-HA in blocking solution overnight at 4 °C, washed with PBS, and incubated with Alexa Fluor 555–conjugated secondary antibody for 2 h at room temperature. After washing with PBS, the cells were mounted with ProLong™ Gold antifade reagent (Thermo Fisher Scientific) and observed with a Nikon confocal microscope.

Expression and purification of recombinant $Tau_{1–441}$ and $Tau_{151–391}$

BL21/pGEX-6P1/$Tau_{1–441}$ and BL21/pGEX-6P1/$Tau_{151–391}$ cultured in LB medium were treated with 0.5 mM isopropyl β-D-thiogalactopyranoside for 3 h at room temperature to induce the protein expression, after which cells were centrifuged at 5,000 × *g* for 10 min at 4 °C. The resulting pellets were resuspended in TBS with 1 mM DTT and a mixture of protease inhibitors for bacteria (Sigma) and probe-sonicated on ice with 70% power for 20 min. The bacterial lysate was adjusted to 1% Triton X-100 and centrifuged at 10,000 × *g* for 15 min. The supernatant was incubated with GSH–Sepharose beads for 1 h at 4 °C. The beads were agitated with PreScission™ Protease (Sigma–Aldrich) in buffer (50 mM Tris-HCl, pH 7.0, 150 mM NaCl, 1 mM EDTA, and 1 mM DTT) to cleave Tau from GST after extensive washing with TBS. Purified Tau was dialyzed against 5 mM MES, pH 6.8, and 0.5 mM EGTA and lyophilized.

Tau aggregation induced by heparin or AD O-Tau in vitro

Recombinant Tau (25 μM) and heparin (0.5 mg/ml) or AD O-Tau (0.53 mg/ml) in 50 μl of PBS containing 50 μM thioflavin T and 1 mM DTT were incubated by shaking at room temperature. Fluorimetry was performed by using a Spectra Max M5 fluorescence spectrophotometer (set at 440-nm excitation/538-nm emission) every 10 min.

Statistical analysis

The GraphPad Prism 6 software was used for statistical analysis. The results were analyzed by one-way ANOVA followed with Tukey's multiple comparisons test or by two-way ANOVA

followed by Sidak's multiple comparisons test for multiple-group analysis.

Data availability

All data are contained within the article.

Acknowledgments—We are thankful to Maureen Marlow for copyediting the manuscript.

Author contributions—J. G., W. X., N. J., L. L., D. C., and F. L. data curation; J. G., W. X., N. J., L. L., and Y. Z. formal analysis; J. G., W. X., N. J., L. L., Y. Z., D. C., and F. L. investigation; C.-X. G., K. I., and F. L. resources; C.-X. G. and K. I. writing-review and editing; F. L. conceptualization; F. L. supervision; F. L. funding acquisition; F. L. validation; F. L. writing-original draft; F. L. project administration.

Funding and additional information—This work was supported in part by funds from New York State Office for People with Developmental Disabilities and Nantong University and by U.S. Alzheimer's Association Grant DSAD-15-363172.

Conflict of interest—The authors declare that they have no conflicts of interest with the contents of this article.

Abbreviations—The abbreviations used are: NFT, neurofibrillary tangle; AD, Alzheimer's disease; AD O-Tau, oligomeric Tau isolated from AD brain tissue; AD P-Tau, hyperphosphorylated and cytosolic Tau isolated from AD brain; aa, amino acid(s); MTBR, microtubule-binding repeat region; GAPDH, glyceraldehyde-3-phosphate dehydrogenase; HMW, high-molecular-weight; LDH, lactate dehydrogenase; RIPA buffer, radioimmunoprecipitation assay buffer; HRP, horseradish peroxidase; rTau, recombinant Tau; HA, hemagglutinin; AEBSF, 4-(2-aminoethyl) benzenesulfonyl fluoride hydrochloride; ANOVA, analysis of variance.

References

1. Braak, H., Braak, E., Grundke-Iqbal, I., and Iqbal, K. (1986) Occurrence of neuropil threads in the senile human brain and in Alzheimer's disease: a third location of paired helical filaments outside of neurofibrillary tangles and neuritic plaques. *Neurosci. Lett.* **65,** 351–355 CrossRef Medline
2. Ballatore, C., Lee, V. M., and Trojanowski, J. Q. (2007) Tau-mediated neurodegeneration in Alzheimer's disease and related disorders. *Nat. Rev. Neurosci.* **8,** 663–672 CrossRef Medline
3. Iqbal, K., Liu, F., and Gong, C. X. (2016) Tau and neurodegenerative disease: the story so far. *Nat. Rev. Neurol.* **12,** 15–27 CrossRef Medline
4. Wang, Y., and Mandelkow, E. (2016) Tau in physiology and pathology. *Nat. Rev. Neurosci.* **17,** 5–21 CrossRef Medline
5. Alafuzoff, I., Adolfsson, R., Grundke-Iqbal, I., and Winblad, B. (1987) Blood–brain barrier in Alzheimer dementia and in non-demented elderly: an immunocytochemical study. *Acta Neuropathol.* **73,** 160–166 CrossRef Medline
6. Arriagada, P. V., Growdon, J. H., Hedley-Whyte, E. T., and Hyman, B. T. (1992) Neurofibrillary tangles but not senile plaques parallel duration and severity of Alzheimer's disease. *Neurology* **42,** 631–639 CrossRef Medline
7. Riley, K. P., Snowdon, D. A., and Markesbery, W. R. (2002) Alzheimer's neurofibrillary pathology and the spectrum of cognitive function: findings from the Nun Study. *Ann. Neurol.* **51,** 567–577 CrossRef Medline
8. Braak, H., and Braak, E. (1991) Neuropathological stageing of Alzheimer-related changes. *Acta Neuropathol.* **82,** 239–259 CrossRef Medline
9. Braak, H., and Braak, E. (1995) Staging of Alzheimer's disease-related neurofibrillary changes. *Neurobiol. Aging* **16,** 271–284 CrossRef Medline
10. Köpke, E., Tung, Y. C., Shaikh, S., Alonso, A. C., Iqbal, K., and Grundke-Iqbal, I. (1993) Microtubule-associated protein Tau. Abnormal phosphorylation of a non-paired helical filament pool in Alzheimer disease. *J. Biol. Chem.* **268,** 24374–24384 Medline
11. Liu, F., Shi, J., Tanimukai, H., Gu, J., Gu, J., Grundke-Iqbal, I., Iqbal, K., and Gong, C.-X. (2009) Reduced *O*-GlcNAcylation links lower brain glucose metabolism and Tau pathology in Alzheimer's disease. *Brain* **132,** 1820–1832 CrossRef Medline
12. Grundke-Iqbal, I., Iqbal, K., Tung, Y. C., Quinlan, M., Wisniewski, H. M., and Binder, L. I. (1986) Abnormal phosphorylation of the microtubule-associated protein Tau (Tau) in Alzheimer cytoskeletal pathology. *Proc. Natl. Acad. Sci. U.S.A.* **83,** 4913–4917 CrossRef Medline
13. Alonso, A. C., Zaidi, T., Grundke-Iqbal, I., and Iqbal, K. (1994) Role of abnormally phosphorylated Tau in the breakdown of microtubules in Alzheimer disease. *Proc. Natl. Acad. Sci. U.S.A.* **91,** 5562–5566 CrossRef Medline
14. Alonso, A. D., Grundke-Iqbal, I., and Iqbal, K. (1996) Alzheimer's disease hyperphosphorylated Tau sequesters normal Tau into tangles of filaments and disassembles microtubules. *Nat. Med.* **2,** 783–787 CrossRef Medline
15. Alonso, A., Zaidi, T., Novak, M., Grundke-Iqbal, I., and Iqbal, K. (2001) Hyperphosphorylation induces self-assembly of Tau into tangles of paired helical filaments/straight filaments. *Proc. Natl. Acad. Sci. U.S.A.* **98,** 6923–6928 CrossRef Medline
16. Clavaguera, F., Bolmont, T., Crowther, R. A., Abramowski, D., Frank, S., Probst, A., Fraser, G., Stalder, A. K., Beibel, M., Staufenbiel, M., Jucker, M., Goedert, M., and Tolnay, M. (2009) Transmission and spreading of tauopathy in transgenic mouse brain. *Nat. Cell Biol.* **11,** 909–913 CrossRef Medline
17. Ahmed, Z., Cooper, J., Murray, T. K., Garn, K., McNaughton, E., Clarke, H., Parhizkar, S., Ward, M. A., Cavallini, A., Jackson, S., Bose, S., Clavaguera, F., Tolnay, M., Lavenir, I., Goedert, M., *et al.* (2014) A novel *in vivo* model of Tau propagation with rapid and progressive neurofibrillary tangle pathology: the pattern of spread is determined by connectivity, not proximity. *Acta Neuropathol.* **127,** 667–683 CrossRef Medline
18. Takeda, S., Wegmann, S., Cho, H., DeVos, S. L., Commins, C., Roe, A. D., Nicholls, S. B., Carlson, G. A., Pitstick, R., Nobuhara, C. K., Costantino, I., Frosch, M. P., Müller, D. J., Irimia, D., and Hyman, B. T. (2015) Neuronal uptake and propagation of a rare phosphorylated high-molecular-weight Tau derived from Alzheimer's disease brain. *Nat. Commun.* **6,** 8490 CrossRef Medline
19. Clavaguera, F., Akatsu, H., Fraser, G., Crowther, R. A., Frank, S., Hench, J., Probst, A., Winkler, D. T., Reichwald, J., Staufenbiel, M., Ghetti, B., Goedert, M., and Tolnay, M. (2013) Brain homogenates from human tauopathies induce Tau inclusions in mouse brain. *Proc. Natl. Acad. Sci. U.S.A.* **110,** 9535–9540 CrossRef Medline
20. Boluda, S., Iba, M., Zhang, B., Raible, K. M., Lee, V. M., and Trojanowski, J. Q. (2015) Differential induction and spread of Tau pathology in young PS19 Tau transgenic mice following intracerebral injections of pathological Tau from Alzheimer's disease or corticobasal degeneration brains. *Acta Neuropathol.* **129,** 221–237 CrossRef Medline
21. Li, L., Jiang, Y., Hu, W., Tung, Y. C., Dai, C., Chu, D., Gong, C. X., Iqbal, K., and Liu, F. (2019) Pathological alterations of Tau in Alzheimer's disease and 3xTg-AD mouse brains. *Mol. Neurobiol.* **56,** 6168–6183 CrossRef Medline
22. Hu, W., Zhang, X., Tung, Y. C., Xie, S., Liu, F., and Iqbal, K. (2016) Hyperphosphorylation determines both the spread and the morphology of Tau pathology. *Alzheimers Dement.* **12,** 1066–1077 CrossRef Medline
23. Dai, C. L., Hu, W., Tung, Y. C., Liu, F., Gong, C. X., and Iqbal, K. (2018) Tau passive immunization blocks seeding and spread of Alzheimer hyperphosphorylated Tau-induced pathology in 3 x Tg-AD mice. *Alzheimers Res Ther* **10,** 13 CrossRef Medline
24. Miao, J., Shi, R., Li, L., Chen, F., Zhou, Y., Tung, Y. C., Hu, W., Gong, C. X., Iqbal, K., and Liu, F. (2019) Pathological Tau from Alzheimer's brain induces site-specific hyperphosphorylation and SDS- and reducing agent-

resistant aggregation of Tau *in vivo*. *Front. Aging Neurosci.* **11,** 34 CrossRef Medline
25. Zilka, N., Filipcik, P., Koson, P., Fialova, L., Skrabana, R., Zilkova, M., Rolkova, G., Kontsekova, E., and Novak, M. (2006) Truncated Tau from sporadic Alzheimer's disease suffices to drive neurofibrillary degeneration *in vivo*. *FEBS Lett.* **580,** 3582–3588 CrossRef Medline
26. Hasegawa, M., Morishima-Kawashima, M., Takio, K., Suzuki, M., Titani, K., and Ihara, Y. (1992) Protein sequence and mass spectrometric analyses of Tau in the Alzheimer's disease brain. *J. Biol. Chem.* **267,** 17047–17054 Medline
27. Yang, L. S., and Ksiezak-Reding, H. (1995) Calpain-induced proteolysis of normal human Tau and Tau associated with paired helical filaments. *Eur. J. Biochem.* **233,** 9–17 CrossRef Medline
28. Seubert, P., Mawal-Dewan, M., Barbour, R., Jakes, R., Goedert, M., Johnson, G. V., Litersky, J. M., Schenk, D., Lieberburg, I., Trojanowski, J. Q., and Lee, V. M.-Y. (1995) Detection of phosphorylated Ser^{262} in fetal Tau, adult Tau, and paired helical filament Tau. *J. Biol. Chem.* **270,** 18917–18922 CrossRef Medline
29. Gamblin, T. C., Chen, F., Zambrano, A., Abraha, A., Lagalwar, S., Guillozet, A. L., Lu, M., Fu, Y., Garcia-Sierra, F., LaPointe, N., Miller, R., Berry, R. W., Binder, L. I., and Cryns, V. L. (2003) Caspase cleavage of Tau: linking amyloid and neurofibrillary tangles in Alzheimer's disease. *Proc. Natl. Acad. Sci. U.S.A.* **100,** 10032–10037 CrossRef Medline
30. Wang, Y., Garg, S., Mandelkow, E. M., and Mandelkow, E. (2010) Proteolytic processing of Tau. *Biochem. Soc. Trans.* **38,** 955–961 CrossRef Medline
31. Zhao, X., Kotilinek, L. A., Smith, B., Hlynialuk, C., Zahs, K., Ramsden, M., Cleary, J., and Ashe, K. H. (2016) Caspase-2 cleavage of Tau reversibly impairs memory. *Nat. Med.* **22,** 1268–1276 CrossRef Medline
32. Zhang, Z., Song, M., Liu, X., Kang, S. S., Kwon, I. S., Duong, D. M., Seyfried, N. T., Hu, W. T., Liu, Z., Wang, J. Z., Cheng, L., Sun, Y. E., Yu, S. P., Levey, A. I., and Ye, K. (2014) Cleavage of Tau by asparagine endopeptidase mediates the neurofibrillary pathology in Alzheimer's disease. *Nat. Med.* **20,** 1254–1262 CrossRef Medline
33. Quinn, J. P., Corbett, N. J., Kellett, K. A. B., and Hooper, N. M. (2018) Tau proteolysis in the pathogenesis of tauopathies: neurotoxic fragments and novel biomarkers. *J. Alzheimers Dis.* **63,** 13–33 CrossRef Medline
34. Ramcharitar, J., Albrecht, S., Afonso, V. M., Kaushal, V., Bennett, D. A., and Leblanc, A. C. (2013) Cerebrospinal fluid Tau cleaved by caspase-6 reflects brain levels and cognition in aging and Alzheimer disease. *J. Neuropathol. Exp. Neurol.* **72,** 824–832 CrossRef Medline
35. Derisbourg, M., Leghay, C., Chiappetta, G., Fernandez-Gomez, F. J., Laurent, C., Demeyer, D., Carrier, S., Buée-Scherrer, V., Blum, D., Vinh, J., Sergeant, N., Verdier, Y., Buee, L., and Hamdane, M. (2015) Role of the Tau N-terminal region in microtubule stabilization revealed by new endogenous truncated forms. *Sci. Rep.* **5,** 9659 CrossRef Medline
36. Novak, M., Kabat, J., and Wischik, C. M. (1993) Molecular characterization of the minimal protease resistant Tau unit of the Alzheimer's disease paired helical filament. *EMBO J.* **12,** 365–370 CrossRef Medline
37. Zhou, Y., Shi, J., Chu, D., Hu, W., Guan, Z., Gong, C. X., Iqbal, K., and Liu, F. (2018) Relevance of phosphorylation and truncation of Tau to the etiopathogenesis of Alzheimer's disease. *Front. Aging Neurosci.* **10,** 27 CrossRef Medline
38. Kovacech, B., and Novak, M. (2010) Tau truncation is a productive posttranslational modification of neurofibrillary degeneration in Alzheimer's disease. *Curr. Alzheimer Res.* **7,** 708–716 CrossRef Medline
39. De Strooper, B. (2010) Proteases and proteolysis in Alzheimer disease: a multifactorial view on the disease process. *Physiol. Rev.* **90,** 465–494 CrossRef Medline
40. Drewes, G., Trinczek, B., Illenberger, S., Biernat, J., Schmitt-Ulms, G., Meyer, H. E., Mandelkow, E. M., and Mandelkow, E. (1995) Microtubule-associated protein/microtubule affinity-regulating kinase (p110mark): a novel protein kinase that regulates Tau-microtubule interactions and dynamic instability by phosphorylation at the Alzheimer-specific site serine 262. *J. Biol. Chem.* **270,** 7679–7688 CrossRef Medline
41. Jeganathan, S., von Bergen, M., Brutlach, H., Steinhoff, H. J., and Mandelkow, E. (2006) Global hairpin folding of Tau in solution. *Biochemistry* **45,** 2283–2293 CrossRef Medline
42. Margittai, M., and Langen, R. (2004) Template-assisted filament growth by parallel stacking of Tau. *Proc. Natl. Acad. Sci. U.S.A.* **101,** 10278–10283 CrossRef Medline
43. Gamblin, T. C., King, M. E., Kuret, J., Berry, R. W., and Binder, L. I. (2000) Oxidative regulation of fatty acid-induced Tau polymerization. *Biochemistry* **39,** 14203–14210 CrossRef Medline
44. Kampers, T., Friedhoff, P., Biernat, J., Mandelkow, E. M., and Mandelkow, E. (1996) RNA stimulates aggregation of microtubule-associated protein Tau into Alzheimer-like paired helical filaments. *FEBS Lett.* **399,** 344–349 CrossRef Medline
45. Goedert, M., Jakes, R., Spillantini, M. G., Hasegawa, M., Smith, M. J., and Crowther, R. A. (1996) Assembly of microtubule-associated protein Tau into Alzheimer-like filaments induced by sulphated glycosaminoglycans. *Nature* **383,** 550–553 CrossRef Medline
46. Sanders, D. W., Kaufman, S. K., DeVos, S. L., Sharma, A. M., Mirbaha, H., Li, A., Barker, S. J., Foley, A. C., Thorpe, J. R., Serpell, L. C., Miller, T. M., Grinberg, L. T., Seeley, W. W., Diamond, M. I. (2014) Distinct tau prion strains propagate in cells and mice and define different tauopathies. *Neuron.* **82,** 1271–1288 CrossRef Medline
47. Wilson, D. M., and Binder, L. I. (1997) Free fatty acids stimulate the polymerization of Tau and amyloid β peptides: *in vitro* evidence for a common effector of pathogenesis in Alzheimer's disease. *Am. J. Pathol.* **150,** 2181–2195 Medline
48. Friedhoff, P., Schneider, A., Mandelkow, E. M., and Mandelkow, E. (1998) Rapid assembly of Alzheimer-like paired helical filaments from microtubule-associated protein Tau monitored by fluorescence in solution. *Biochemistry* **37,** 10223–10230 CrossRef Medline
49. Zhang, W., Falcon, B., Murzin, A. G., Fan, J., Crowther, R. A., Goedert, M., and Scheres, S. H. (2019) Heparin-induced Tau filaments are polymorphic and differ from those in Alzheimer's and Pick's diseases. *eLife* **8,** e43584 CrossRef Medline
50. Jeganathan, S., Hascher, A., Chinnathambi, S., Biernat, J., Mandelkow, E. M., and Mandelkow, E. (2008) Proline-directed pseudo-phosphorylation at AT8 and PHF1 epitopes induces a compaction of the paperclip folding of Tau and generates a pathological (MC-1) conformation. *J. Biol. Chem.* **283,** 32066–32076 CrossRef Medline
51. von Bergen, M., Friedhoff, P., Biernat, J., Heberle, J., Mandelkow, E. M., and Mandelkow, E. (2000) Assembly of Tau protein into Alzheimer paired helical filaments depends on a local sequence motif (^{306}VQIVYK^{311}) forming β structure. *Proc. Natl. Acad. Sci. U.S.A.* **97,** 5129–5134 CrossRef Medline
52. Mukrasch, M. D., Biernat, J., von Bergen, M., Griesinger, C., Mandelkow, E., and Zweckstetter, M. (2005) Sites of Tau important for aggregation populate β-structure and bind to microtubules and polyanions. *J. Biol. Chem.* **280,** 24978–24986 CrossRef Medline
53. Rissman, R. A., Poon, W. W., Blurton-Jones, M., Oddo, S., Torp, R., Vitek, M. P., LaFerla, F. M., Rohn, T. T., and Cotman, C. W. (2004) Caspase-cleavage of Tau is an early event in Alzheimer disease tangle pathology. *J. Clin. Invest.* **114,** 121–130 CrossRef Medline
54. Mandelkow, E., von Bergen, M., Biernat, J., and Mandelkow, E. M. (2007) Structural principles of Tau and the paired helical filaments of Alzheimer's disease. *Brain Pathol.* **17,** 83–90 CrossRef Medline
55. Alonso, A. D., Zaidi, T., Novak, M., Barra, H. S., Grundke-Iqbal, I., and Iqbal, K. (2001) Interaction of Tau isoforms with Alzheimer's disease abnormally hyperphosphorylated Tau and *in vitro* phosphorylation into the disease-like protein. *J. Biol. Chem.* **276,** 37967–37973 CrossRef Medline
56. Abraha, A., Ghoshal, N., Gamblin, T. C., Cryns, V., Berry, R. W., Kuret, J., and Binder, L. I. (2000) C-terminal inhibition of Tau assembly *in vitro* and in Alzheimer's disease. *J. Cell Sci.* **113,** 3737–3745 Medline
57. Alonso, A. D. C., Mederlyova, A., Novak, M., Grundke-Iqbal, I., and Iqbal, K. (2004) Promotion of hyperphosphorylation by frontotemporal dementia Tau mutations. *J. Biol. Chem.* **279,** 34873–34881 CrossRef Medline
58. Arai, T., Miklossy, J., Klegeris, A., Guo, J. P., and McGeer, P. L. (2006) Thrombin and prothrombin are expressed by neurons and glial cells and accumulate in neurofibrillary tangles in Alzheimer disease brain. *J. Neuropathol. Exp. Neurol.* **65,** 19–25 CrossRef Medline

59. Arai, T., Guo, J. P., and McGeer, P. L. (2005) Proteolysis of non-phosphorylated and phosphorylated Tau by thrombin. *J. Biol. Chem.* **280,** 5145–5153 CrossRef Medline
60. Marcinkiewicz, M., and Seidah, N. G. (2000) Coordinated expression of β-amyloid precursor protein and the putative β-secretase BACE and α-secretase ADAM10 in mouse and human brain. *J. Neurochem.* **75,** 2133–2143 CrossRef Medline
61. Lammich, S., Kojro, E., Postina, R., Gilbert, S., Pfeiffer, R., Jasionowski, M., Haass, C., and Fahrenholz, F. (1999) Constitutive and regulated α-secretase cleavage of Alzheimer's amyloid precursor protein by a disintegrin metalloprotease. *Proc. Natl. Acad. Sci. U.S.A.* **96,** 3922–3927 CrossRef Medline
62. Gatta, L. B., Albertini, A., Ravid, R., and Finazzi, D. (2002) Levels of β-secretase BACE and α-secretase ADAM10 mRNAs in Alzheimer hippocampus. *Neuroreport* **13,** 2031–2033 CrossRef Medline
63. Yuan, X. Z., Sun, S., Tan, C. C., Yu, J. T., and Tan, L. (2017) The role of ADAM10 in Alzheimer's disease. *J. Alzheimers Dis.* **58,** 303–322 CrossRef Medline
64. Saftig, P., and Lichtenthaler, S. F. (2015) The α secretase ADAM10: a metalloprotease with multiple functions in the brain. *Prog. Neurobiol.* **135,** 1–20 CrossRef Medline
65. Chu, D., and Liu, F. (2019) Pathological changes of Tau related to Alzheimer's disease. *ACS Chem. Neurosci.* **10,** 931–944 CrossRef Medline
66. Henriksen, K., Wang, Y., Sørensen, M. G., Barascuk, N., Suhy, J., Pedersen, J. T., Duffin, K. L., Dean, R. A., Pajak, M., Christiansen, C., Zheng, Q., and Karsdal, M. A. (2013) An enzyme-generated fragment of Tau measured in serum shows an inverse correlation to cognitive function. *PLoS One* **8,** e64990 CrossRef Medline
67. Neergaard, J. S., Dragsbæk, K., Christiansen, C., Karsdal, M. A., Brix, S., and Henriksen, K. (2018) Two novel blood-based biomarker candidates measuring degradation of Tau are associated with dementia: a prospective study. *PLoS One* **13,** e0194802 CrossRef Medline
68. Inekci, D., Henriksen, K., Linemann, T., Karsdal, M. A., Habib, A., Bisgaard, C., Eriksen, F. B., and Vilholm, O. J. (2015) Serum fragments of Tau for the differential diagnosis of Alzheimer's disease. *Curr. Alzheimer Res.* **12,** 829–836 CrossRef Medline
69. Henriksen, K., Byrjalsen, I., Christiansen, C., and Karsdal, M. A. (2015) Relationship between serum levels of Tau fragments and clinical progression of Alzheimer's disease. *J. Alzheimers Dis.* **43,** 1331–1341 CrossRef Medline
70. Grundke-Iqbal, I., Iqbal, K., Quinlan, M., Tung, Y. C., Zaidi, M. S., and Wisniewski, H. M. (1986) Microtubule-associated protein Tau: a component of Alzheimer paired helical filaments. *J. Biol. Chem.* **261,** 6084–6089 Medline
71. Luna-Muñoz, J., Chávez-Macías, L., García-Sierra, F., and Mena, R. (2007) Earliest stages of Tau conformational changes are related to the appearance of a sequence of specific phospho-dependent Tau epitopes in Alzheimer's disease. *J. Alzheimers Dis.* **12,** 365–375 CrossRef Medline
72. Flores-Rodríguez, P., Ontiveros-Torres, M. A., Cárdenas-Aguayo, M. C., Luna-Arias, J. P., Meraz-Ríos, M. A., Viramontes-Pintos, A., Harrington, C. R., Wischik, C. M., Mena, R., Florán-Garduño, B., and Luna-Muñoz, J. (2015) The relationship between truncation and phosphorylation at the C-terminus of Tau protein in the paired helical filaments of Alzheimer's disease. *Front. Neurosci.* **9,** 33 Medline
73. Guillozet-Bongaarts, A. L., Garcia-Sierra, F., Reynolds, M. R., Horowitz, P. M., Fu, Y., Wang, T., Cahill, M. E., Bigio, E. H., Berry, R. W., and Binder, L. I. (2005) Tau truncation during neurofibrillary tangle evolution in Alzheimer's disease. *Neurobiol Aging* **26,** 1015–1022 CrossRef Medline
74. Lyu, X. J., Li, Z. H., Li, X., Zeng, W. L., Yang, P., Lin, Q. X., Zheng, J. Y., Du, X. L., Gu, Y. Z., Zhao, Y. Q., Xie, R. S., Liu, T., Lin, H. L., and Ma, W. J. (2017) Commuting mode specific exposure to PM(2.5) in urban area of Guangzhou. *Zhonghua Liu Xing Bing Xue Za Zhi* **38,** 309–313 Medline
75. Basurto-Islas, G., Luna-Muñoz, J., Guillozet-Bongaarts, A. L., Binder, L. I., Mena, R., and García-Sierra, F. (2008) Accumulation of aspartic acid 421- and glutamic acid 391-cleaved Tau in neurofibrillary tangles correlates with progression in Alzheimer disease. *J. Neuropathol. Exp. Neurol.* **67,** 470–483 CrossRef Medline
76. Wang, J. Z., Grundke-Iqbal, I., and Iqbal, K. (2007) Kinases and phosphatases and Tau sites involved in Alzheimer neurofibrillary degeneration. *Eur. J. Neurosci.* **25,** 59–68 CrossRef Medline
77. Wischik, C. M., Novak, M., Thøgersen, H. C., Edwards, P. C., Runswick, M. J., Jakes, R., Walker, J. E., Milstein, C., Roth, M., and Klug, A. (1988) Isolation of a fragment of Tau derived from the core of the paired helical filament of Alzheimer disease. *Proc. Natl. Acad. Sci. U.S.A.* **85,** 4506–4510 CrossRef Medline
78. Amadoro, G., Serafino, A. L., Barbato, C., Ciotti, M. T., Sacco, A., Calissano, P., and Canu, N. (2004) Role of N-terminal Tau domain integrity on the survival of cerebellar granule neurons. *Cell Death Differ.* **11,** 217–230 CrossRef Medline
79. Amadoro, G., Ciotti, M. T., Costanzi, M., Cestari, V., Calissano, P., and Canu, N. (2006) NMDA receptor mediates Tau-induced neurotoxicity by calpain and ERK/MAPK activation. *Proc. Natl. Acad. Sci. U.S.A.* **103,** 2892–2897 CrossRef Medline
80. Corsetti, V., Amadoro, G., Gentile, A., Capsoni, S., Ciotti, M. T., Cencioni, M. T., Atlante, A., Canu, N., Rohn, T. T., Cattaneo, A., and Calissano, P. (2008) Identification of a caspase-derived N-terminal Tau fragment in cellular and animal Alzheimer's disease models. *Mol. Cell Neurosci.* **38,** 381–392 CrossRef Medline
81. Park, S. Y., and Ferreira, A. (2005) The generation of a 17 kDa neurotoxic fragment: an alternative mechanism by which Tau mediates β-amyloid–induced neurodegeneration. *J. Neurosci.* **25,** 5365–5375 CrossRef Medline
82. Xia, D., Li, C., and Götz, J. (2015) Pseudophosphorylation of Tau at distinct epitopes or the presence of the P301L mutation targets the microtubule-associated protein Tau to dendritic spines. *Biochim. Biophys. Acta* **1852,** 913–924 CrossRef Medline
83. Padmanabhan, P., Martínez-Mármol, R., Xia, D., Götz, J., and Meunier, F. A. (2019) Frontotemporal dementia mutant Tau promotes aberrant Fyn nanoclustering in hippocampal dendritic spines. *eLife* **8,** e45040 CrossRef Medline
84. Pei, J. J., Braak, E., Braak, H., Grundke-Iqbal, I., Iqbal, K., Winblad, B., and Cowburn, R. F. (1999) Distribution of active glycogen synthase kinase 3β (GSK-3β) in brains staged for Alzheimer disease neurofibrillary changes. *J. Neuropathol. Exp. Neurol.* **58,** 1010–1019 CrossRef Medline

ASBMB